



## 저작자표시-비영리-변경금지 2.0 대한민국

이용자는 아래의 조건을 따르는 경우에 한하여 자유롭게

- 이 저작물을 복제, 배포, 전송, 전시, 공연 및 방송할 수 있습니다.

다음과 같은 조건을 따라야 합니다:



저작자표시. 귀하는 원저작자를 표시하여야 합니다.



비영리. 귀하는 이 저작물을 영리 목적으로 이용할 수 없습니다.



변경금지. 귀하는 이 저작물을 개작, 변형 또는 가공할 수 없습니다.

- 귀하는, 이 저작물의 재이용이나 배포의 경우, 이 저작물에 적용된 이용허락조건을 명확하게 나타내어야 합니다.
- 저작권자로부터 별도의 허가를 받으면 이러한 조건들은 적용되지 않습니다.

저작권법에 따른 이용자의 권리는 위의 내용에 의하여 영향을 받지 않습니다.

이것은 [이용허락규약\(Legal Code\)](#)을 이해하기 쉽게 요약한 것입니다.

[Disclaimer](#)

# Analysis and design of the acoustic metasurface unit structure and applying for stealth technology

WooHoon Jung

Department of Mechanical Engineering

Ulsan National Institute of Science and Technology

# Analysis and design of the acoustic metasurface unit structure and applying for stealth technology

A thesis/dissertation submitted to  
Ulsan National Institute of Science and Technology  
in partial fulfillment of the  
requirements for the degree of  
Master of Science

WooHoon Jung

05. 31. 2021

Approved by

---

Advisor

Joo Hwan Oh

Analysis and Design of the Acoustic Metasurface Unit Structure and Applying  
for Stealth Technology

Woo Hoon Jung

This certifies that the thesis/dissertation of WooHoon Jung is approved.

05. 31. 2021

signature

---

Advisor: Joo Hwan Oh

signature

---

Thesis Committee Member#1 : SungYoub Kim

signature

---

Thesis Committee Member#2 : WonJae Choi

## Abstract

Wave is very closely related to our life in the form of light, vibration, and sound. In general, wave moves according to the laws established in the natural world, but using metasurfaces or metamaterials we can realize a completely new wave system. Metasurface is a technology that creates a new wave phenomenon that can't be seen in the natural world by periodically arranging structure that smaller than the wavelength of the wave. The biggest feature of metasurface and metamaterial is that they can control the propagating direction of the wave and also realize the phenomenon such as negative refraction [1-2] or negative reflection [3]. In the past, many studies have been conducted only in the field of optics, but recently there are a lot of researches to implement a new method of vibration/noise reduction technology by applying metasurface and metamaterial technologies to the Elastic/Acoustic fields.

This thesis is try to introduce the technology that dissipating the acoustic energy by applying the metasurface. Through structure design, it is possible to control the wave propagating direction by adjusting the "Phase Gradient" which is the ratio of phase change according to the direction of wave traveling. The magnitude of the phase gradient can be adjusted through the periodicity of the structure, and larger the value of phase gradient, more rapid movement of the wave can be realized. The energy of the wave can be dissipated by using a technology that converting to the surface wave which moves along the surface of the structure, and moreover mode conversion to the higher order by diffraction can be generated. In the process of mode conversion, wave stays on the surface of the structure for a certain period time [4] and moves along the unit structure. As a result, it takes additional time for reflection to occur in metasurface, while reflection instantly occur on the normal surface. During the conversion process, the energy of the wave is dissipated by the loss factor of a medium and as a result, the wave energy reflected from the metasurface is significantly reduced than before the incident.

The acoustic metasurface technology in this thesis focuses on controlling the propagation direction of acoustic wave and energy dissipation. These tecnology will be helpful to develop the new way of solving a lot of acoustic problems such as sound problem in air and ultrasonic issues in the water.



## Contents

I. Introduction-----	1
1.1 Background of metamaterial and metasurface-----	1
1.2 Research objectives and verification process-----	1
II. Theoretical & mathematical development-----	3
2.1 Wave equation in acoustic field-----	3
2.2 Snell's law and phase gradient-----	7
2.3 Two points method and structure design of metasurface-----	8
2.4 Higher order mode conversion by wave diffraction-----	11
2.5 Acoustic impedance of PDMS and water-----	13
III. Manipulating the reflection angle-----	15
3.1 Theoretical development and structure design-----	15
3.1.1 Verify reflection angle-----	15
3.1.2 Negative reflection-----	17
3.2 Simulation results -----	18
3.2.1 Verify reflection angle-----	18
3.2.2 Negative reflection-----	19
3.3 Experimental validation-----	20
3.3.1 Experimental materials and setup-----	20
3.3.2 Verify reflection angle-----	24
3.3.3 Negative reflection -----	25

IV. Energy dissipation-----	27
4.1 Theoretical development and structure design-----	27
4.1.1 Design the large phase gradient metasurface-----	27
4.2 Simulation-----	28
4.2.1 Simulation setting-----	28
4.2.2 Frequency response simulation result-----	30
4.2.3 Transient simulation result-----	32
4.3 Experimental validation -----	36
4.3.1 Experimental results-----	36
V. Conclusions-----	40
VI. References-----	41
VII. Acknowledgement-----	42



## List of figures

Fig. 2-1 Net flow through control volume

Fig. 2-2 Phase shift on metasurface

Fig. 2-3 Two points method for measuring phase gradient in extended duct structure

Fig. 2-4 Phase change following the unit length  $L$

Fig. 2-5 Mechanism of higher order conversion by diffraction and time delay

Fig. 2-6 Reflection and Transmission at the boundary interface of two different materials

Fig. 2-7 Acoustic wave transmission through PDMS from water without reflection

Fig3-1. (a) Meta structure unit using for two points method. (b) Phase gradient graph according to change of unit length. (c) Selected unit length to realize the  $0^\circ$  incidence wave reflect to  $15^\circ$

Fig3-2. (a) Meta structure unit using for two points method. (b) Phase gradient graph according to change of unit length. (c) Selected unit length to realize the  $0^\circ$  incidence wave reflect to  $30^\circ$

Fig. 3-3 (a) Meta structure unit using for two points method. (b) Phase gradient graph according to change of unit length. (c) Selected unit length to realize the  $0^\circ$  incidence wave reflect to  $45^\circ$

Fig. 3-4 (a) Meta structure unit using for two points method. (b) Phase gradient graph according to change of unit length. (c) Selected unit length to realize the  $-20^\circ$  incidence wave reflect to  $60^\circ$

Fig. 3-5  $0^\circ$  incident wave reflect to (a)  $15^\circ$  (b)  $30^\circ$  (c)  $45^\circ$

Fig. 3-6 (a) Incident wave with  $-20^\circ$  (b) Reflection wave with  $60^\circ$

Fig. 3-7 Experimental equipment and data process

Fig. 3-8 Experimental setting of equipment and specimens

Fig. 3-9 Fabricated metasurface of metasurface manipulating  $0^\circ$  incidence wave to reflect in  $15^\circ, 30^\circ, 45^\circ$

Fig. 3-10 Fabricated metasurface of negative reflection

Fig. 3-11 Image of data measured by probe (a) Incidence, (b) Reflection  $15^\circ$  (c) Reflection  $30^\circ$  (d) Reflection  $45^\circ$

Fig. 3-12 Image of data measured by probe (a) Incidence  $-20^\circ$  (b) Reflection  $60^\circ$

Fig. 4-1 (a) Meta structure unit using for two points method (b) Phase gradient graph according to change of unit length (c) Selected unit length to realize the higher order mode conversion by diffraction

Fig. 4-2 Setting of the simulation

Fig. 4-3 (a) Parameter setting for the pressure wave speed (b) Variable setting for shear wave speed

Fig. 4-4 (a) Component list of COMSOL Multiphysics (b) Material setting for the normal solid materials (c) Material setting for PDMS by using the wave speed

Fig. 4-5 (a) Incidence wave to normal surface (b) Reflection wave from normal surface

Fig. 4-6 (a) Incidence wave to meta surface (b) Reflection wave from meta surface

Fig. 4-7 (a) Meta structure unit using for two points method (b) Measured incidence/reflection wave at the probe

Fig. 4-8 (a) Raw data measured at probe (b) FFT for total wave (c) FFT for incidence wave (d) FFT for reflection wave

Fig. 4-9 (a) Meta structure unit using for two points method (b) Simulation result of time delay occurred between normal surface and metasurface.

Fig. 4-10 (a) Raw data measured at probe (b) FFT for total wave (c) FFT for incidence wave (d) FFT for reflection wave

Fig. 4-11 Experimental result of time delay between normal surface and metasurface

Fig. 4-12 Fabricated meta surface combined with PDMS

Fig. 4-13 (a) Raw data from experiment with normal surface (b) FFT result of incidence wave (c) FFT result of reflection wave

Fig. 4-14 (a) Raw data from experiment with meta surface (b) FFT result of incidence wave (c) FFT result of reflection wave

## List of tables

Table. 2-1 Table of the conversion to the higher mode by diffraction

## 1. Introduction

### 1.1 Background of metamaterial and metasurface

Metamaterial is a technology that can realize wave phenomena that do not exist in the natural world by periodically arranging artificially designed structures. Metamaterials are being actively researched in the fields of Electromagnetic, Elastic wave, and Acoustic wave. The biggest feature is that the motion of the wave is not dependent on the properties of the material, but influenced by the structure. Metamaterials realize new wave motion according to its structure, size, direction and arrangement.

It is possible to implement a bandgap [5] phenomenon in which a wave does not proceed even though a medium exists in a specific frequency band. Using these properties, we can approach to the vibration/noise problem in a new way. However, since metamaterials must be periodically arranged along the direction of wave propagation, there is a structural limitation in size. The proposed technology to overcome this limitation is the metasurface.

Metasurface is a technology that proposed to improve the structural limitation of metamaterials, and it is possible to implements a new wave system by periodically arranging structures smaller than the wavelength of the wave. Wave has the property of diffraction limit [6-7], which act as if they interact with a single substance when they interact with structures of less than half a wavelength. For this reason, the structure of the metasurface must be made of a structure smaller than the half wavelength of the wave.

The biggest feature of the metasurface is that it controls the propagating direction of the wave by adjusting the phase. Using these characteristics, it is possible to implement “Negative refraction” or “Negative reflection” that overcome the “Snell’s Law” which defines the motion of general wave and also we can control the directivity of the wave. Recently, new technologies using metasurface in the fields of optics, vibration, and acoustic are being actively studied.

### 1.2 Research objectives and verification process

In this thesis, a study was conducted about controlling the propagation direction of the acoustic wave and energy dissipation by using the metasurface. An acoustic wave is a wave phenomenon in which energy is transmitted by contraction and expansion of a medium. Speed and impedance characteristic of the wave vary according to the type of medium, and the most well-known acoustic wave is the “Sound” that move in the air or water.

Electromagnetic wave is actively used as communication method due to the limitation of sound that wave can't travel far and dissipate quickly in the air. However, in water, the absorption rate of electromagnetic wave is very high and rather, the sound wave is transmitted farther. For this reason, sound wave is actively used as a means of communication in the water. As a security problem, there has been a need for a stealth technology capable of avoiding acoustic detection. Stealth technology, which aims to prevent the acoustic wave return to the source to transmit information, can be implemented in two ways. First, by manipulating the reflection degree when the acoustic wave bumped against the surface of the object, decrease the amount of wave returning to the source. Second, method that makes the object appear to be non-exist by preventing reflection from occurring on the surface of the object. In this thesis, we intend to develop stealth technology by implementing these two phenomena using metasurface.

By manipulating the phase gradient of acoustic wave with metasurface, we could realize not only controlling the reflection angle but also design the anechoic structure that reflection does not occur. Process of the research are as follow

Step 1: Theoretical approach and structural design considering the phase gradient

Step 2: Verification of result through simulation

Step 3: Verification through experiment with metasurface

Through this process, we could realize the “Negative reflection” and “Anechoic structure”. The final performance of the metasurface was dissipating 96% of the incident wave energy. The result of this study would be useful to develop the stealth technology that free from sound detection in water and also provide a new method of handling the sound/noise problem.

## 2. Theoretical & Mathematical Development

### 2.1 Wave equation in Acoustic field

In this section, general wave equation in Acoustic field will be introduces. Before deriving the general wave equation, following equations and definitions will be commonly used

$\vec{u}$  = particle velocity of a fluid element

$$\vec{u} = u_x \hat{x} + u_y \hat{y} + u_z \hat{z} \quad (2.1)$$

$\rho$  = instantaneous density at  $(x, y, z)$

$\rho_0$  = equilibrium density at  $(x, y, z)$

$s$  = condensation at  $(x, y, z)$

$$s = \frac{(\rho - \rho_0)}{\rho_0} \quad (2-2)$$

$\rho - \rho_0 = \rho_0 s$  = acoustic density at  $(x, y, z)$

$\mathbb{P}$  = instantaneous pressure at  $(x, y, z)$

$\mathbb{P}_0$  = equilibrium pressure at  $(x, y, z)$

$p$  = acoustic pressure at  $(x, y, z)$

$$p = \mathbb{P} - \mathbb{P}_0 \quad (2-3)$$

$c$  = speed of acoustic wave in the fluid

To derive the wave equation in acoustic field, we will use these 3 equations

- 1) Equation of state
- 2) Equation of continuity
- 3) Euler's Equation

- 1) Equation of state

The equation of state (ideal gas law)

$$PV = nRT \quad (2-4)$$

As it is adiabatic process, pressure  $P$  is a function of  $\rho$

$$P = C\rho \quad \left( C = \frac{\partial P}{\partial \rho} = \text{constant} \right) \quad (2-5)$$

$$P - P_0 = B \frac{\rho - \rho_0}{\rho_0} \quad \left( B = \rho_0 \frac{\partial P}{\partial \rho} \right) \quad (2-6)$$

$$P - P_0 = Bs \quad \left( s = \frac{\rho - \rho_0}{\rho_0} \right) \quad (2-7)$$

## 2) Equation of continuity

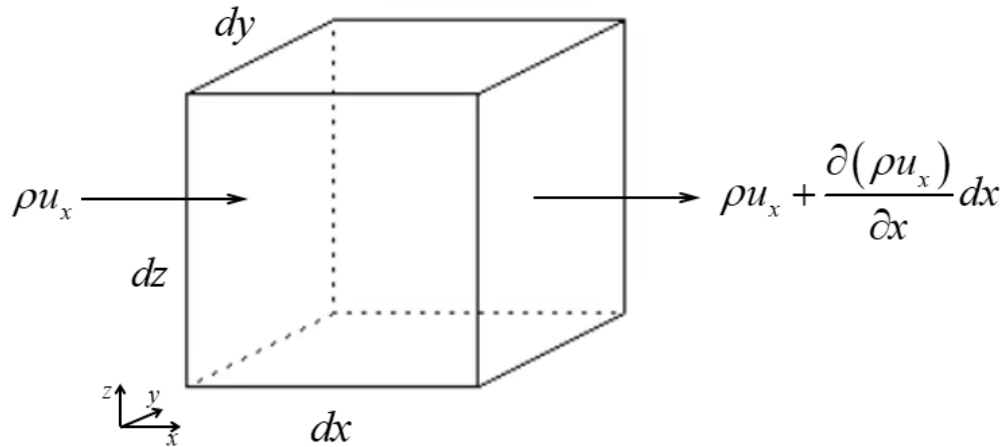


Fig. 2-1 Net flow through control volume

Net influx of mass in to the volume in x direction

$$\left[ \rho u_x - \left( \rho u_x + \frac{\partial(\rho u_x)}{\partial x} dx \right) \right] dydz = - \frac{\partial(\rho u_x)}{\partial x} dV \quad (2-8)$$

When consider not only x direction but also y, z direction, the total influx will be

$$- \left( \frac{\partial(\rho u_x)}{\partial x} + \frac{\partial(\rho u_y)}{\partial y} + \frac{\partial(\rho u_z)}{\partial z} \right) dV = - \nabla \cdot (\rho \vec{u}) dV \quad (2-9)$$

The rate of mass increase in the volume is  $\left(\frac{\partial \rho}{\partial t}\right)dV$  and it must be same with total influx

$$\frac{\partial \rho}{\partial t} + \nabla \cdot (\rho \vec{u}) = 0 \quad (2-10)$$

If we write  $\rho = \rho_0(1 + s)$  and use some assumptions “ $\rho_0$  is sufficiently weak function of time”, “ $u \times s$  is so small”,

$$\rho_0 \frac{\partial s}{\partial t} + \nabla \cdot (\rho_0 \vec{u}) = 0 \quad (2-11)$$

and if  $\rho_0$  is only a weak function of space

$$\frac{\partial s}{\partial t} + \nabla \cdot \vec{u} = 0 \quad (2-12)$$

### 3) Euler's equation

Net force  $d\vec{f}$  on element of fluid will accelerate it according to Newton's 2<sup>nd</sup> law.

$$d\vec{f} = \vec{a} dm \text{ (Assumption: No viscosity)} \quad (2-13)$$

Net force in x direction

$$df_x = \left[ \mathbb{P} - \left( \mathbb{P}_0 + \frac{\partial \mathbb{P}}{\partial x} dx \right) \right] dydz = -\frac{\partial \mathbb{P}}{\partial x} dV \quad (2-14)$$

When we consider gravity and y, z direction

$$d\vec{f} = -\nabla \cdot \mathbb{P} dV + \vec{g} \rho dV \quad (2-15)$$

To express the acceleration of the fluid element

$$\vec{u}(x + u_x dt, y + u_y dt, z + u_z dt, t + dt) = \vec{u}(x, y, z, t) + \frac{\partial \vec{u}}{\partial x} u_x dt + \frac{\partial \vec{u}}{\partial y} u_y dt + \frac{\partial \vec{u}}{\partial z} u_z dt + \frac{\partial \vec{u}}{\partial t} dt \quad (2-16)$$



$$\vec{a} = \lim_{dt \rightarrow 0} \frac{\vec{u}(x+u_x dt, y+u_y dt, z+u_z dt, t+dt) - \vec{u}(x, y, z, t)}{dt} = \frac{\partial \vec{u}}{\partial t} + u_x \frac{\partial \vec{u}}{\partial x} + u_y \frac{\partial \vec{u}}{\partial y} + u_z \frac{\partial \vec{u}}{\partial z} \quad (2-17)$$

If we define

$$\vec{u} \cdot \nabla \equiv u_x \frac{\partial}{\partial x} + u_y \frac{\partial}{\partial y} + u_z \frac{\partial}{\partial z} \quad (2-18)$$

$\vec{a}$  can be written as

$$\vec{a} = \frac{\partial \vec{u}}{\partial t} + (\vec{u} \cdot \nabla) \vec{u} \quad (2-19)$$

As  $dm$  of the element is  $\rho dV$ , substitute this expression in Eq. (2-13)

$$-\nabla \mathbb{P} + \vec{g} \rho = \rho \left( \frac{\partial \vec{u}}{\partial t} + (\vec{u} \cdot \nabla) \vec{u} \right) \quad (2-20)$$

In the case of no acoustic excitations,  $\vec{g} \rho_0 = \nabla \mathbb{P}_0$  and thus  $\nabla \mathbb{P} = \nabla p + \vec{g} \rho_0$

Eq. (2-20) become

$$-\frac{1}{\rho_0} \nabla p + \vec{g} s = (1+s) \left( \frac{\partial \vec{u}}{\partial t} + (\vec{u} \cdot \nabla) \vec{u} \right) \quad (2-21)$$

With assumptions that  $|\vec{g} s| \ll \left| \frac{\nabla p}{\rho_0} \right|$  that  $|s| \ll 1$  and  $|(\vec{u} \cdot \nabla) \vec{u}| \ll \left| \frac{\partial \vec{u}}{\partial t} \right|$  then

$$\rho_0 \frac{\partial \vec{u}}{\partial t} = -\nabla p \quad (2-22)$$

#### 4) Wave equation in Acoustic field

We can derive the Wave equation by using Eq. (2-7), Eq. (2-11) and Eq. (2-22)

First, take the divergence of Eq. (2-22)

$$\nabla \cdot \left( \rho_0 \frac{\partial \vec{u}}{\partial t} \right) = -\nabla^2 p \quad (2-23)$$

Take the time derivative of Eq. (2-11)

$$\rho_0 \frac{\partial^2 s}{\partial t^2} + \nabla \cdot \left( \rho_0 \frac{\partial \vec{u}}{\partial t} \right) = 0 \quad (2-24)$$

Substitute divergence term in Eq. (2-23) with Eq. (2-24)

$$\nabla^2 p = \rho_0 \frac{\partial^2 s}{\partial t^2} \quad (2-25)$$

By using Eq. (2-7) we can derive

$$\nabla^2 p = \frac{1}{c^2} \frac{\partial^2 p}{\partial t^2} \quad (2-26)$$

## 2.2 Snell's Law and phase gradient

Snell's law defines the motion of a wave at the boundary of different media by using the characteristic that the speed of a wave varies depending on the medium. Through this equation, it is possible to know the movement of the wave in the refraction and reflection phenomena that occur when the wave moves from one medium to another. The general Snell's law is written as Eq. (2-27)

$$k \sin \theta_i = k \sin \theta_r \quad (2-27)$$

$\theta_i$  is incidence angle,  $\theta_r$  is reflection angle, and  $k$  is the wave number which is described as Eq. (28)

$$k = \frac{2\pi f}{c}, (f = \text{frequency}, c = \text{wave speed}) \quad (2-28)$$

According to Eq. (2-27), it can be seen that in a general plane, the angle of incidence and the angle of reflection are always the same.

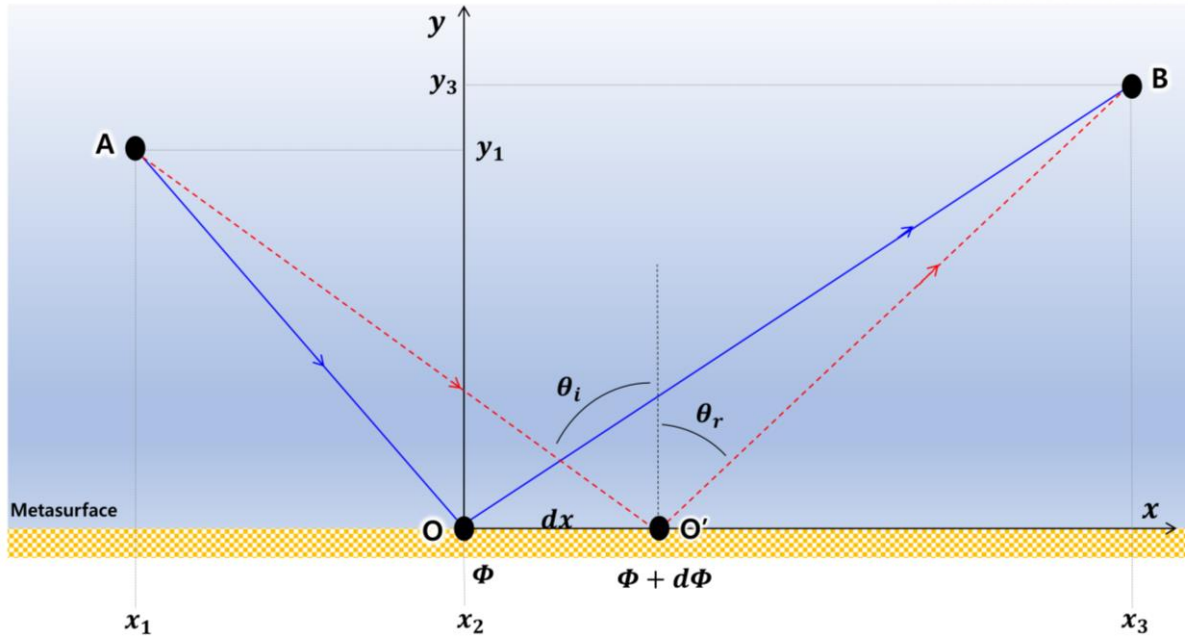


Fig. 2-2 Phase shift on metasurface

However, metasurface is constructed by microstructures that periodically arranged and it causes a phase shift to the incidence wave. Due to this effect, Snell's law changes to differently. Let's induce an new form of Snell's law that can be applied on metasurface.

Fig 2-2 is describing the incidence wave and reflection wave from metasurface. According to Fermat's principle, waves tend to travel along the shortest distance, and if this is explained in terms of phase, it can be said that they propagate along the direction in which the phase change is minimized. In other words, even when the wave propagates along the direction AO'B which is slightly different from original path, the phase change is same as the AOB. If you express it with a formula, you can understand it more intuitively. The phase changed along the AOB can be expressed as Eq. (2-29)

$$k \sin \theta_i \times (x_2 - x_1) + k \cos \theta_i \times y_1 + \Phi + k \sin \theta_r \times (x_3 - x_2) + k \cos \theta_r \times y_3 \quad (2-29)$$

Phase change along the AO'B can be expressed as Eq. (2-30)

$$k \sin \theta_i \times (x_2 + dx - x_1) + k \cos \theta_i \times y_1 + (\Phi + d\Phi) + k \sin \theta_r \times (x_3 - x_2 - dx) + k \cos \theta_r \times y_3 \quad (2-30)$$

Since the phase changed along AOB and the phase changed along AO'B are the same, it is summarized as Eq. (2-31)

$$k \sin \theta_i - k \sin \theta_r = \Psi \quad (2-31)$$

$\Psi$  is a Phase gradient and it can be expressed as  $\frac{d\Phi}{dx}$ . It means a value obtained by differentiating the phase difference expressed in the metasurface according to the direction of progression. In this way, by periodically arranging microstructures in the metasurface, the reflection angle of the wave can be manipulated through the phase gradient effect.

### 2.3 Two points method and structure design of metasurface

In previous section, it was confirmed that the phase gradient plays an essential role in controlling the direction of the reflected wave in metasurface, and it was found that the phase gradient is occurred through the phase difference caused by microstructures. In general, the structure used to control the phase difference uses a complex structure such as Coiling-up space, Helmholtz-resonator, and Membrane-type structure, however in this study an extended duct structure described in Fig. 2-3 was used by consideration of durability and productivity.

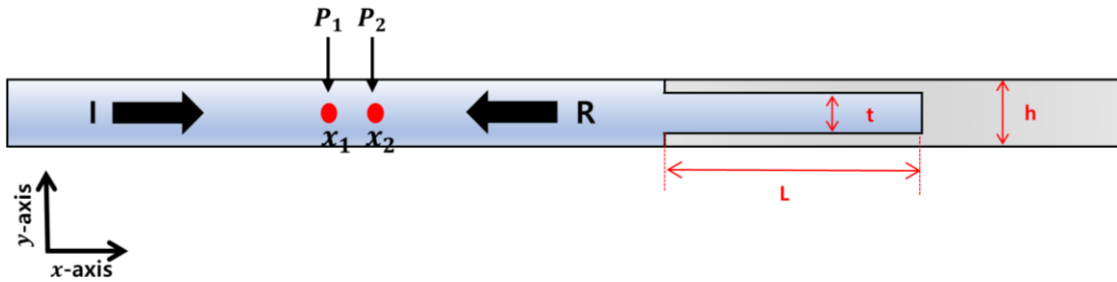


Fig. 2-3 Two points method for measuring phase gradient in extended duct structure

In the unit structure as shown in Fig 2-3, we can manipulate the phase gradient by using the phase difference caused by changing the length  $L$  of unit structure. In this study, the phase change ratio of the reflected wave to the incident wave was calculated using a method called the two points method. It is a method that calculates the phase difference of the reflected wave separately in a simulation where the incident wave and the reflected wave are mixed. As shown in Fig 2-3, this is a method of calculating the phase difference using the pressure data measured at two different points  $x_1$  and  $x_2$ . First, it is assumed that the incident wave and the reflected wave have the relationship as the Eq. (2-32)

$$\begin{aligned} I &= I_0 e^{i(\omega t - kx)} \\ R &= R_0 e^{i(\omega t + kx)} \end{aligned} \quad (2-32)$$

In this case, the pressure measured at  $x_1$  and  $x_2$  has the following values.

$$\begin{aligned} P_1 &= I_0 e^{i(\omega t - kx_1)} + R_0 e^{i(\omega t + kx_1)} \\ P_2 &= I_0 e^{i(\omega t - kx_2)} + R_0 e^{i(\omega t + kx_2)} \end{aligned} \quad (2-33)$$

It can be expressed as matrix like Eq. (2-34)

$$\begin{bmatrix} e^{-ikx_1} & e^{ikx_1} \\ e^{-ikx_2} & e^{ikx_2} \end{bmatrix} \begin{bmatrix} I_0 \\ R_0 \end{bmatrix} \times e^{i\omega t} = \begin{bmatrix} P_1 \\ P_2 \end{bmatrix} \quad (2-34)$$

After taking the inverse matrix on both sides, it can be expressed like Eq. (2-35)

$$\begin{aligned} I_0 \times e^{i\omega t} &= \frac{P_1 e^{ikx_2} - P_2 e^{ikx_1}}{2 \sin[k(x_1 - x_2)]} \\ R_0 \times e^{i\omega t} &= \frac{-P_1 e^{-ikx_2} + P_2 e^{-ikx_1}}{2 \sin[k(x_1 - x_2)]} \end{aligned} \quad (2-35)$$

As a result, the phase change occurring in the microstructure can be calculated as follows.

$$\Phi = \frac{R_0}{I_0} \quad (2-36)$$

In summary, the relationship between length L from Fig 2-3 and  $\Phi$  from Eq. (2-36) is shown as Fig 2-4. As the size of L changes, the relative phase difference between the incident wave and the reflected wave changes, and the final design plan of the metasurface can be derived through selecting suitable microstructure that creates the desired phase gradient by the designer.

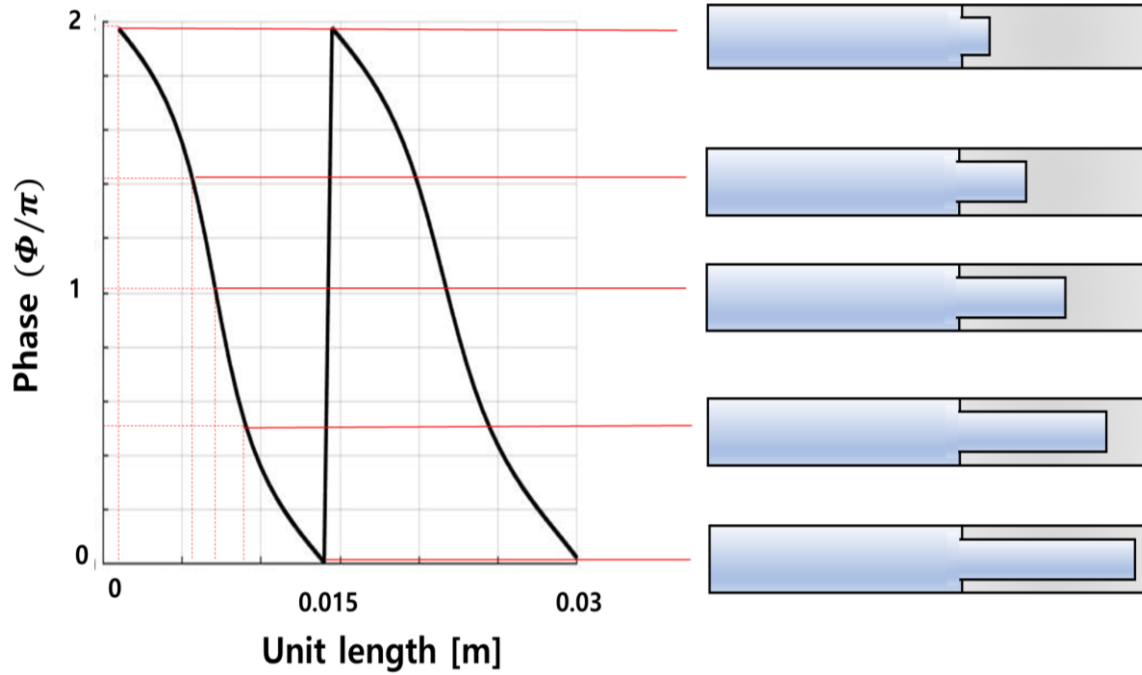


Fig. 2-4 Phase change following the unit length L

$$\Psi = \frac{\Delta \Phi}{h} \quad (2-37)$$

Eq. (2-37) is the definition of phase gradient, which means the ratio of phase change occurring every slit interval  $h$ . For example, in Fig 2-4, a metasurface was designed by selecting a structure with a phase difference of  $0.5\pi \text{ rad}$  per  $h$ .

#### 2.4 Higher order mode conversion by wave diffraction

We found that the angle of the reflected wave can be controlled by adjusting the phase gradient. As the phase gradient increases, the amount of change in the reflection angle increases, and conversion to a surface wave can be implemented. However, if the phase gradient increases beyond specific limit, a slightly different phenomenon occurs than the previous, which is the higher order mode conversion by diffraction. When an acoustic wave enters the metasurface with a high phase gradient, the supercell acts as a new source due to the effect of diffraction. After that, only the appropriate higher order mode is reflected out according to the model and size of the supercell, and these phenomena change the Snell's law to the new way as Eq. (2-38).

$$k \sin \theta_i - k \sin \theta_r = \Psi - nG_d \quad (2-38)$$

$G_d$  in Eq. (2-38) is reciprocal lattice vector which has the same value with  $\Psi$  and  $n$  is the number

of mode. Schematic of this as a table is shown in Table. 2-1.

I) $n = 0$	$\theta_r = \sin^{-1}[\sin \theta_i + \frac{\Psi}{k}] > 90^\circ$	Surface Wave
II) $n = 1$	$\theta_r = \theta_i$	Reflection
III) $n = 2$	$\theta_r = \sin^{-1}[\sin \theta_i - G_d] > 90^\circ$	Surface Wave
IV) $n = 3$	$\theta_r = \sin^{-1}[\sin \theta_i - 2G_d] > 90^\circ$	Surface Wave
V) $n = \dots$	$\theta_r = \sin^{-1}[\sin \theta_i - 3G_d] > 90^\circ$	Surface Wave

Table. 2-1 Table of the conversion to the higher mode by diffraction

As shown in Table. 2-1, when an acoustic wave is incident on a metasurface that has high phase gradient, the order of formation varies depending on the size of  $\theta_i$ . In this study, since the case of normal incidence was considered, it can be confirmed that if  $\theta_i = 0^\circ$ , all acoustic waves other than the first order mode cannot be reflected and only the first order mode is reflected as shown in Table. 2-1. The most important phenomenon in this process is that it takes a certain time during mode conversion.

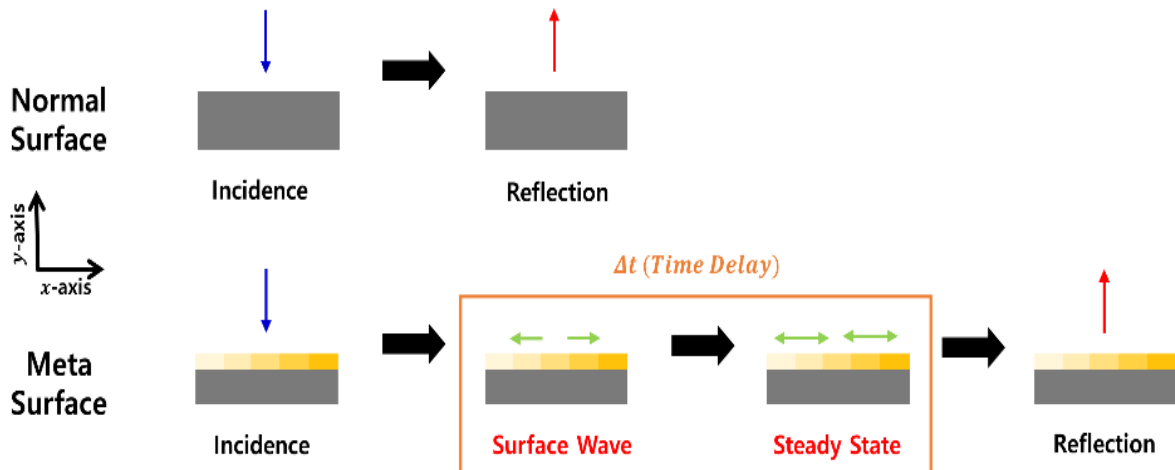


Fig. 2-5 Mechanism of higher order conversion by diffraction and time delay

As shown in Fig. 2-5, the incident acoustic wave is reflected directly from the normal surface, whereas in the metasurface with high phase gradient, the incident acoustic wave is converted to a surface wave and then reflected again after going through the steady state. Therefore, in metasurfaces

with high phase gradient, acoustic wave reflection occurs slightly more slowly than normal surfaces. Thickness could be confirmed through simulations and experiments.

## 2.5 Acoustic impedance of PDMS and water

Every material has its own acoustic impedance. This is a factor that determines the motion of acoustic waves in different media, and reflectance ratio and refractive ratio vary according to their relative sizes. Acoustic impedance is usually expressed as  $Z$ , and the definition is equal to Eq. (2-39).

$$Z = \rho c = \sqrt{\rho \cdot E} \quad (2-39)$$

$\rho$  is density of material,  $c$  is wave speed in media,  $E$  is Young's modulus and unit is "rayl"

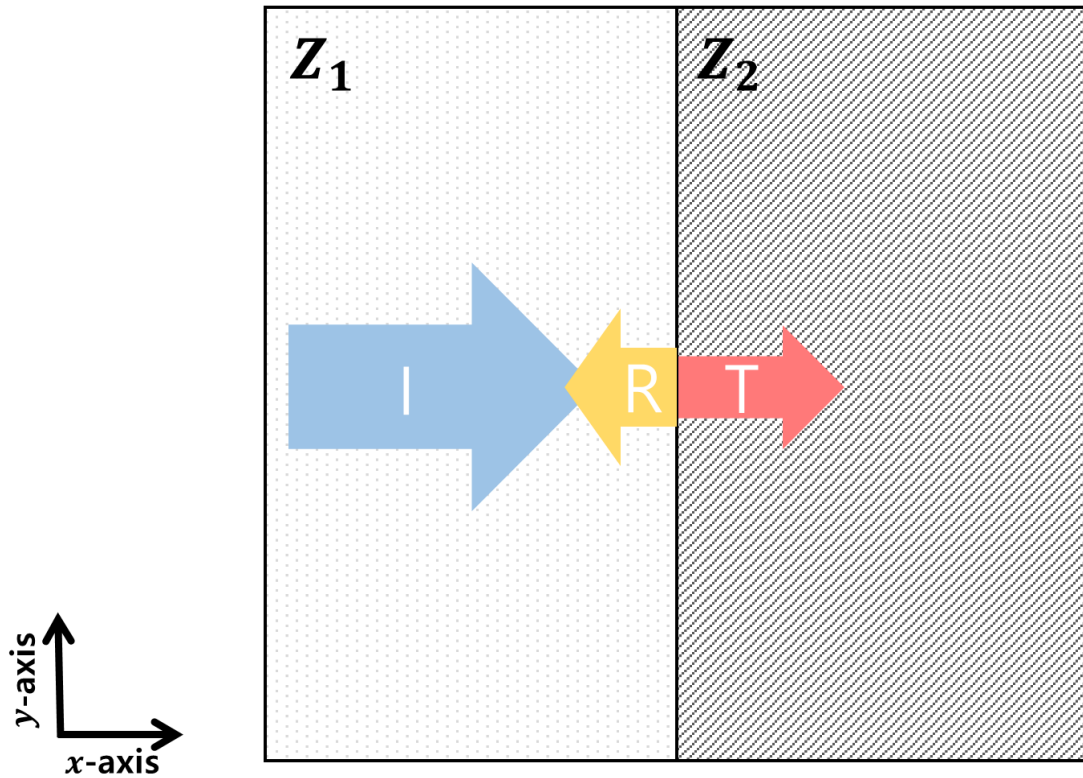


Fig. 2-6 Reflection and Transmission at the boundary interface of two different materials

$$R = \frac{Z_2 - Z_1}{Z_2 + Z_1} \quad T = \frac{2Z_1}{Z_2 + Z_1} \quad (2-40)$$

Fig 2-6 is describing the reflected and transmitted waves generated due to the difference when acoustic waves are incident on the interface of media with different impedances. Depending on the impedance difference, the amount of reflected and transmitted energy is different, and the relationship is equal to Eq. (2-40). This study deals with the movement of acoustic wave in water,



and the acoustic impedance of water is  $1.48 \text{ Mrayl}$ . The technology that dissipating the acoustic energy will be realized by using a PDMS [8-9] which have a similar acoustic impedance with the water. Acoustic impedance of the PDMS is  $1 \text{ Mrayl}$ , and according to Eq. (2-40), about 19% of reflection is going to be occur. However, since this is a ratio of amplitude, when translate it to energy ratio, it can be seen that only about 4% of the energy is reflected and the remaining 96% of the energy is transmitted. This could be confirmed through the verification step through simulation as Fig 2-7 and also through experimentation.

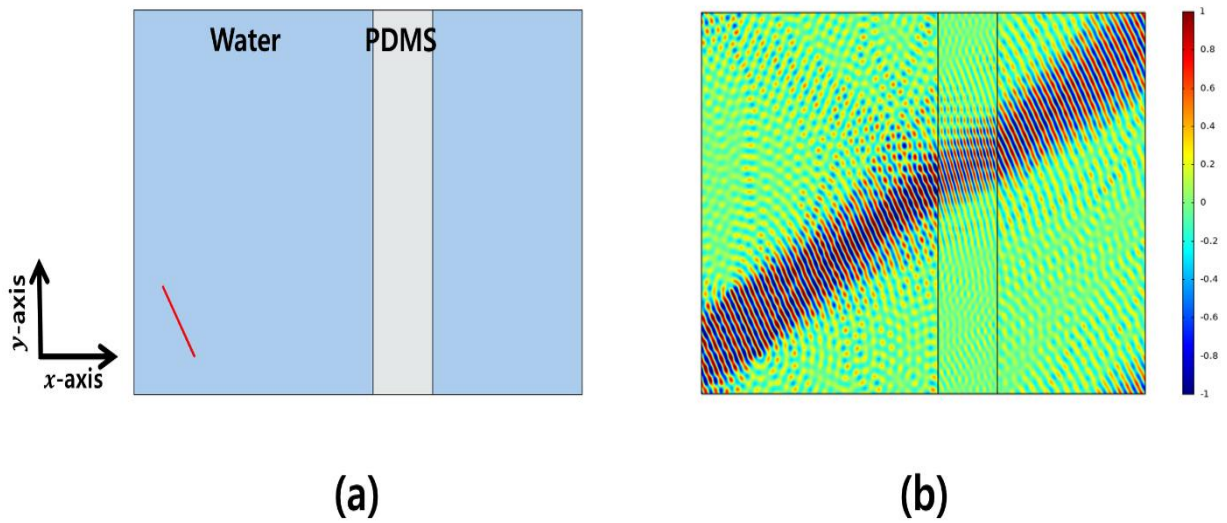


Fig. 2-7 Acoustic wave transmission through PDMS from water without reflection

### 3. Manipulating the reflection angle

#### 3.1 Theoretical development and structure design

The biggest feature of the metasurface is that it can control the direction of travel by using the phase of the wave. We can use the metasurface to adjust the angle of reflection and refraction, and by using this, we can implement phenomena that do not occur in the existing natural world such as energy focusing [10] and negative refraction/reflection. In this section, based on the theory described in the previous sections 2.1, 2.2, and 2.3, the metasurface that can manipulate the angle of reflection will be described. Applying the theory, we will design a structure where reflection occurs at a desired angle.

##### 3.1.1 Verify reflection angle

First, in order to implement the simplest reflection angle control, I would like to design a metasurface that allows the acoustic wave incident at  $0^\circ$  to be reflected at  $15^\circ, 30^\circ, 45^\circ$ . The conditions in this study are water with a velocity of 1484m/s as a medium and a frequency of 50kHz. According to Eq. (2-31), to manipulate the  $0^\circ$  incidence wave reflect to  $15^\circ$ ,  $\Psi$  must be 54.79rad/m and by using relation that  $\Psi = \frac{d\Phi}{dx}$  and  $d\Phi = 2\pi$ , we can easily find out that  $dx=0.12\text{m}$ . In other words, it is sufficient to design a meta structure that generates a  $2\pi$  phase difference every 0.12m. At this time, number of division of 0.12m depends on the intention of the designer. If it is too thin, scattering may occur due to structural deformation, and if it is too thick, performance of the meta structure may not be exhibited properly, so it is important to find out the optimal structure following the conditions.

Let's design the metasurface that reflect the  $0^\circ$  incidence acoustic wave to  $15^\circ, 30^\circ, 45^\circ$ . Using two points method that described in section 2.3, we can find out that phase change ratio according to the length of each meta unit is shown as Fig 3-1(b), Fig 3-2(b), and Fig 3-3(b).

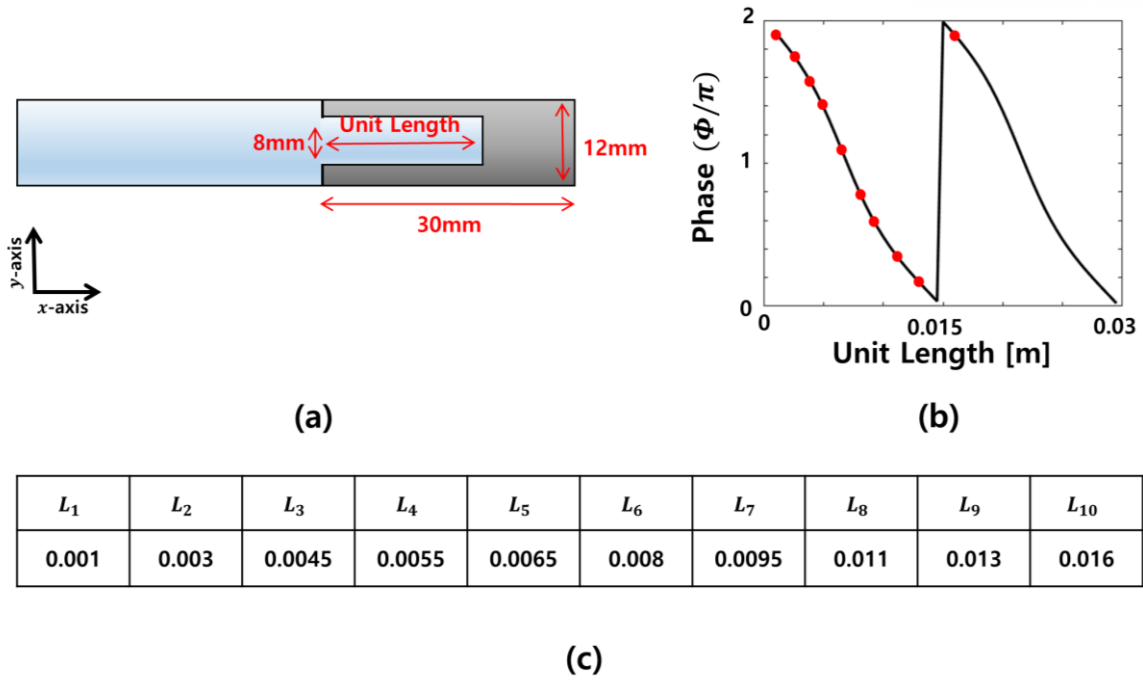


Fig. 3-1 (a) Meta structure unit using for two points method. (b) Phase gradient graph according to change of unit length. (c) Selected unit length to realize the  $0^\circ$  incidence wave reflect to  $15^\circ$

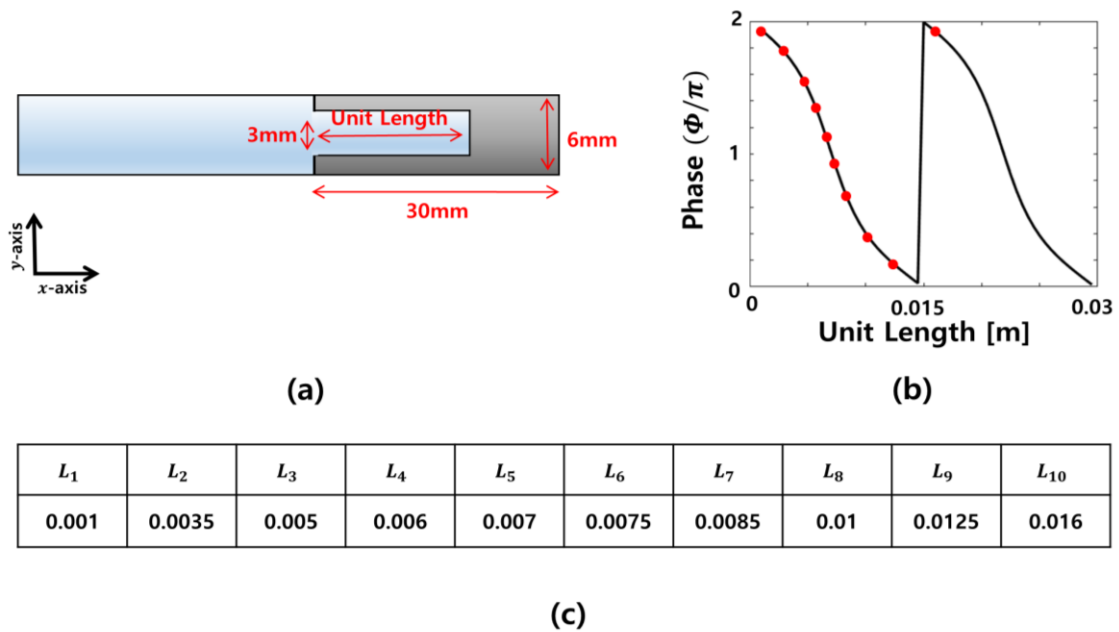


Fig. 3-2 (a) Meta structure unit using for two points method. (b) Phase gradient graph according to change of unit length. (c) Selected unit length to realize the  $0^\circ$  incidence wave reflect to  $30^\circ$

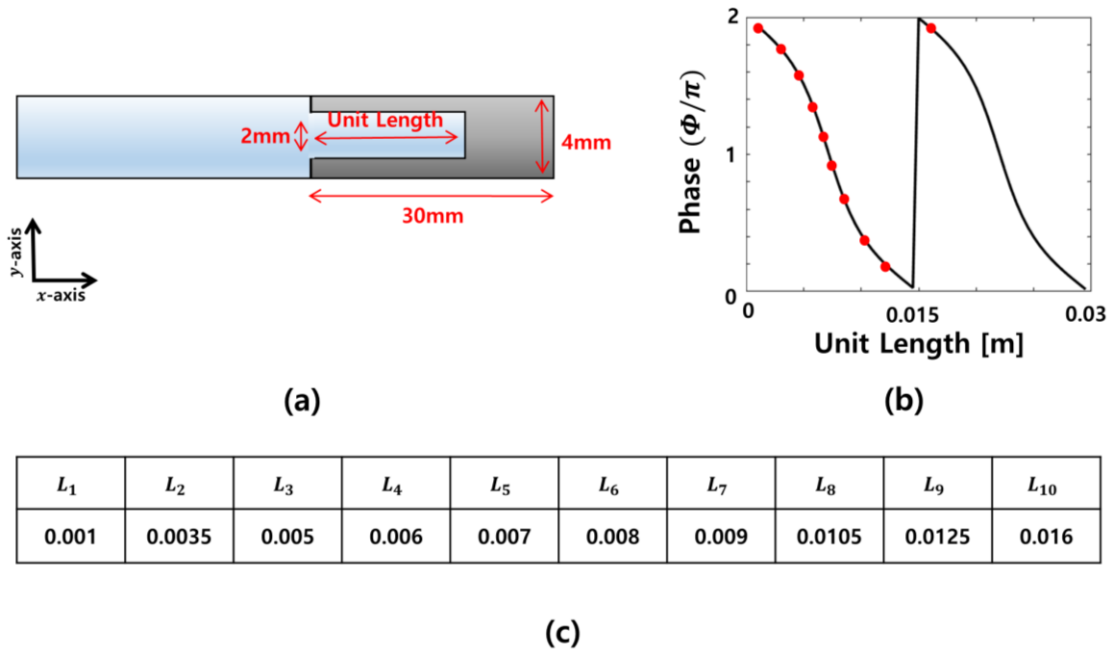


Fig. 3-3 (a) Meta structure unit using for two points method. (b) Phase gradient graph according to change of unit length. (c) Selected unit length to realize the  $0^\circ$  incidence wave reflect to  $45^\circ$

Fig 3-1 shows the process of designing meta structure that reflect  $0^\circ$  incident wave to  $15^\circ$ . The phase change rate of the reflected wave to the incident wave was measured by changing the unit length gradually 0.0005m in the unit structure shown in Fig 3-1(a). As a result, the rate of phase change according to the unit length can be expressed as a graph in Fig 3-1(b). The Fig 3-1(c) is the result of dividing final meta unit geometrical length that total supercell changing  $2\pi$  of phase. Fig 3-2 and Fig 3-3 are the process of designing a meta structure that reflects  $0^\circ$  incident wave to  $30^\circ$  and  $45^\circ$  respectively.

### 3.1.2 Negative reflection

In this section, we will design a meta structure that can give more dynamic changes by using the reflection angle control technology that described earlier. This is a negative reflection phenomenon that does not occur in the general plane. In this paper, in order to show extreme phenomena, we designed a meta structure that manipulate the  $-20^\circ$  incident wave reflect to  $60^\circ$ . By using designing step described in section 3.1.1, we can easily find out that  $\Psi$  of metasurface should be 255.7rad/m and  $dx = 0.025\text{m}$  to control the  $-20^\circ$  incident wave reflect to  $60^\circ$ . Considering various factor, designer decided to use five 5mm

thickness of meta unit structures and we can easily follow the step through Fig 3-4. From these results, it can be seen that higher phase gradient is required for a more dramatic and dynamic angular change.

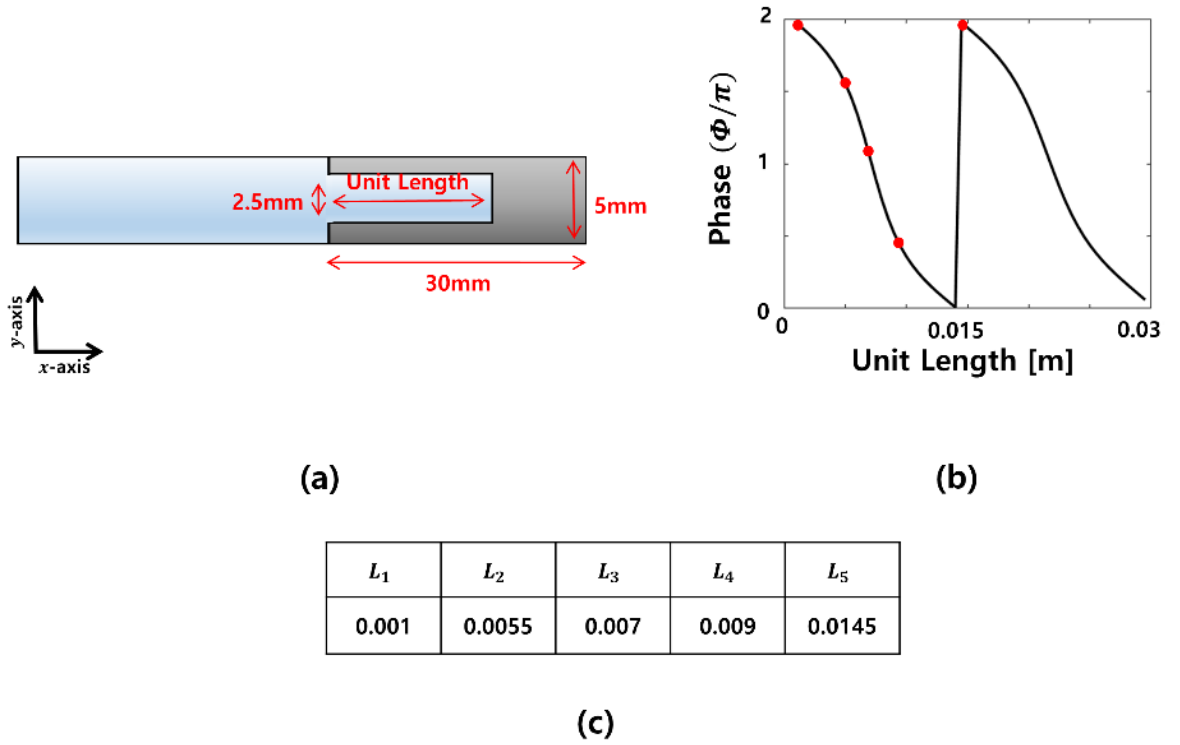


Fig. 3-4 (a) Meta structure unit using for two points method. (b) Phase gradient graph according to change of unit length. (c) Selected unit length to realize the  $-20^\circ$  incidence wave reflect to  $60^\circ$

### 3.2 Simulation results

Based on the theoretical approach in section 3.1, the results were confirmed through simulation. It was able to verify the phenomenon that  $0^\circ$  incident wave reflect to  $15^\circ, 30^\circ, 45^\circ$  and  $-20^\circ$  incident wave reflect to  $60^\circ$ .

#### 3.2.1 Verify reflection angle

Fig 3-5 is the result of confirming through simulation the phenomenon that that  $0^\circ$  incident wave reflect to  $15^\circ, 30^\circ, 45^\circ$ . In this figure, incident wave was removed and only reflection wave was plotted to clarify the result.

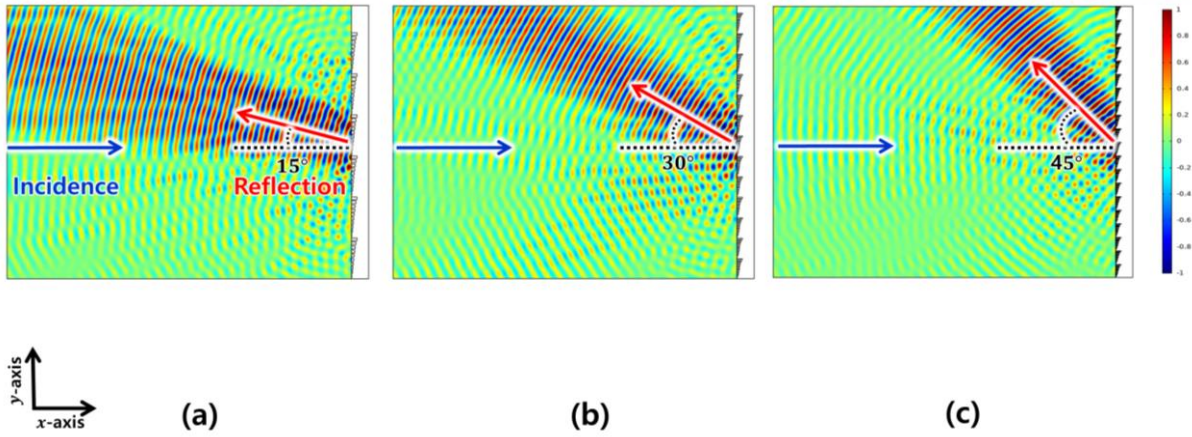


Fig. 3-5  $0^\circ$  incident wave reflect to (a)  $15^\circ$  (b)  $30^\circ$  (c)  $45^\circ$

As can be seen from Fig 3-5, the metasurface designed in section 3.1 operates well and it can manipulate the reflection wave in a desired direction.

### 3.2.2 Negative reflection

Fig 3-6 shows simulation result of negative reflection phenomenon that  $-20^\circ$  incident wave reflect to  $60^\circ$ . It is very meaningful achievement that the negative reflection phenomenon, which was not observed in the natural world, was actually implemented through structural design.

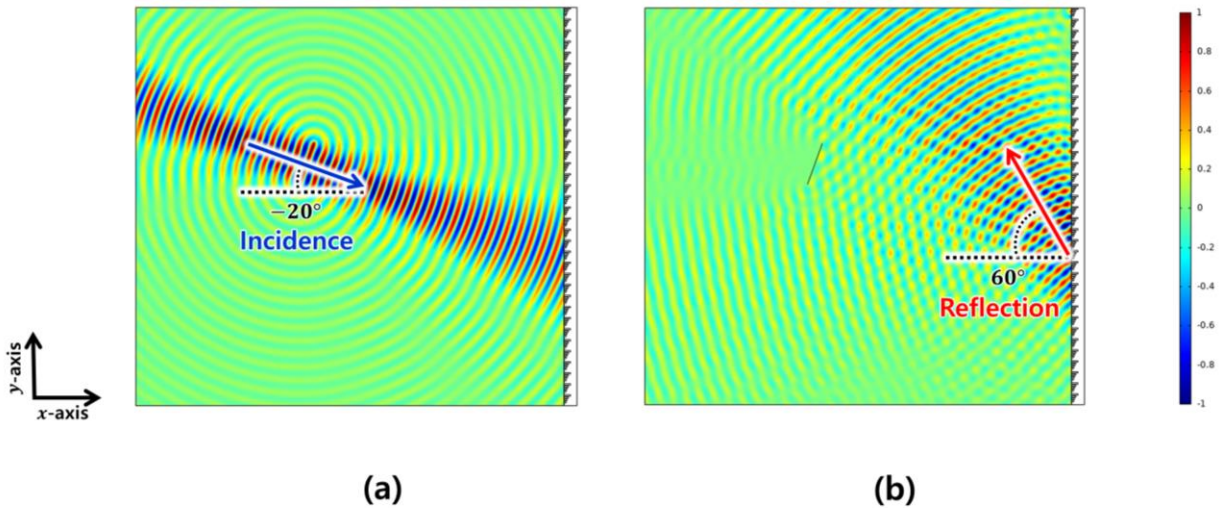


Fig. 3-6 (a) Incident wave with  $-20^\circ$  (b) Reflection wave with  $60^\circ$



### 3.3 Experimental validation

In this section, I will verify the experimental result based on the theoretical approach and the result of simulation in previous section. Although the actual experiment is more influenced by external factors than the simulation, errors may occur, but I tried to increase the accuracy by establishing the best environment. Let me explain the experimental equipment and experimental settings first, and then explain the results of each experiment.

#### 3.3.1 Experimental materials and setup

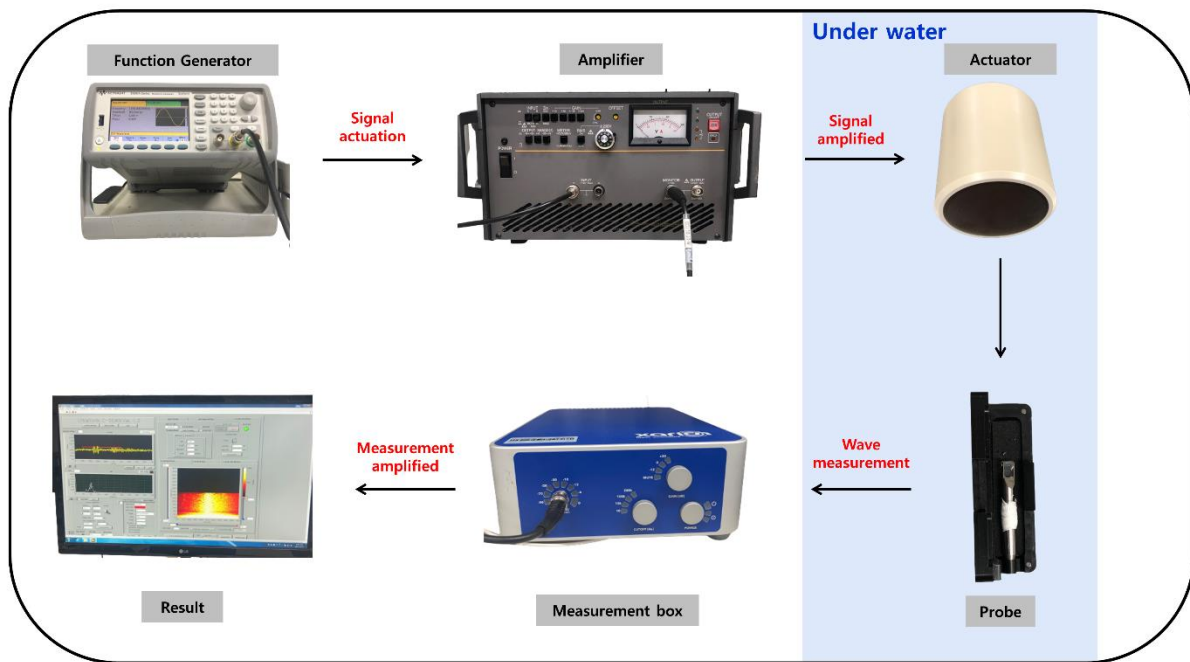


Fig. 3-7 Experimental equipment and data process

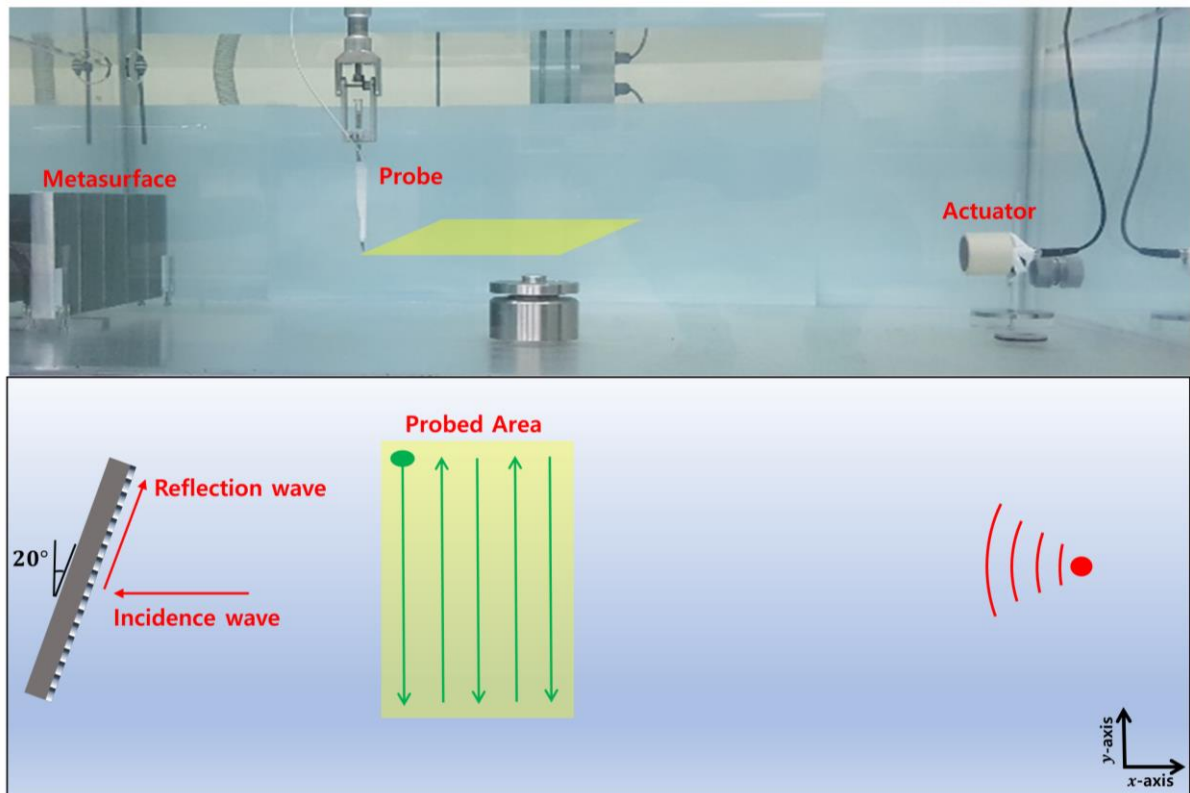


Fig. 3-8 Experimental setting of equipment and specimens

As shown in Fig 3-7, the signal generated from the function generator is amplified while passing through the amplifier and then excite through the actuator. In the probed area of Fig 3-8, probe measured the pressure of incidence/reflection wave following the imaginary point. The measured result value can be visualized through the related program. The structure at the center of Fig 3-8 is a structure that is necessary for a rotating body test and cannot be removed due to the limitation of the overall testing equipment. However, the experiment was conducted after confirming that structure do not affect to this experiment through a verification experiment.

Water is a medium with many variables such as nonlinearity and changes in the velocity of acoustic waves with temperature. In order to increase the accuracy of the experiment, the experiment was conducted after all air inside the tank was drained for several days by receiving the water from the tank in advance. Because the impedances of air and water are different, and air bubbles formed on the surface of the structure and the experimental equipment will affect the movement of acoustic waves, which can act as an error factor.

#### <Materials>

Function Generator : It is an experimental equipment that makes an electrical signal. It serves



to designate all the characteristics of the waveform required for excitation such as waveform, frequency, amplitude, burst, and cycle.

**Amplifier :** There are cases where the amplitude is insufficient only by the function generator, and at that time, it plays the role of amplifying the value. You can decide how many times to amplify through setting, and you can find the optimal magnification by looking at the amplitude value measured in real time. In addition, if an appropriate amplification value is specified in consideration of the loss factor of the medium or the sensitivity of the probe, a better experimental result can be obtained.

**Actuator :** Converting electrical signals that have passed through the function generator and amplifier into acoustic waves to be generated. Since there is a frequency band in charge of each actuator, it is important to use an appropriate actuator that meets the conditions.

**Probe:** Since it is a very sensitive laboratory equipment, it must be put in water before the experiment and optimized to adjust to the temperature. It scans the area designated by the researcher, measures the amplitude of the acoustic wave at a virtual point, and then extracts data.

**Measurement box :** Amplify and filter the data measured by the probe. It increases the accuracy of the experiment by measuring only the frequency of the desired band through the low pass/high pass filter.

**Result :** The data measured through the probe is received through a program designed with LabView. One point measurement and image conversion using scanned data can be performed, and the actual probe movement can be controlled, thus serving as the overall head quarter of the experiment.

#### <Setup>

Experiment was conducted by placing metasurface on the left side of the tank and an actuator on the right side. At the experiment that  $0^\circ$  incident wave reflect to  $15^\circ, 30^\circ, 45^\circ$ , metasurface and actuator arranged parallel to each other. However, at the experiment of  $-20^\circ$  incident wave reflect to  $60^\circ$ , for the limitation of the tank size, the metasurface was rotated to implement the  $-20^\circ$  incidence condition. Because, if the actuator is moved, it was difficult to obtain an accurate measurement value when considering the location of the probed area. In addition, the most important part in conduction the experiment is that the distance between the metasurface and the actuator is to be kept far away. Due to the

characteristics of the acoustic wave, it spreads as a circular wave, so the distance between the metasurface and the actuator is distanced to maximize the characteristics of the plane wave.

#### <Specimen metasurface>

Let's manufacture the metasurface designed in section 3.1 and verify its performance through experiment. Fig 3-9 is the manufactured metasurface that manipulating the  $0^\circ$  incidence wave to reflect in  $15^\circ, 30^\circ, 45^\circ$ . Fig 3-10 is the metasurface for manipulating the  $-20^\circ$  incidence wave to reflect in  $60^\circ$ , which is negative reflection.

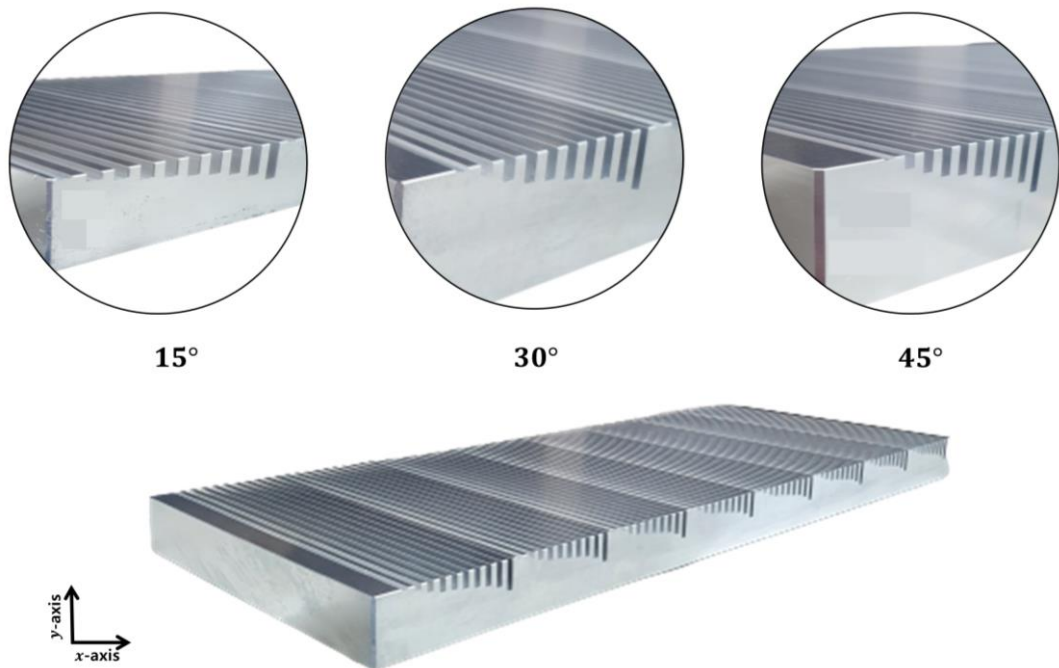


Fig. 3-9 Fabricated metasurface of metasurface manipulating  $0^\circ$  incidence wave to reflect in  $15^\circ, 30^\circ, 45^\circ$

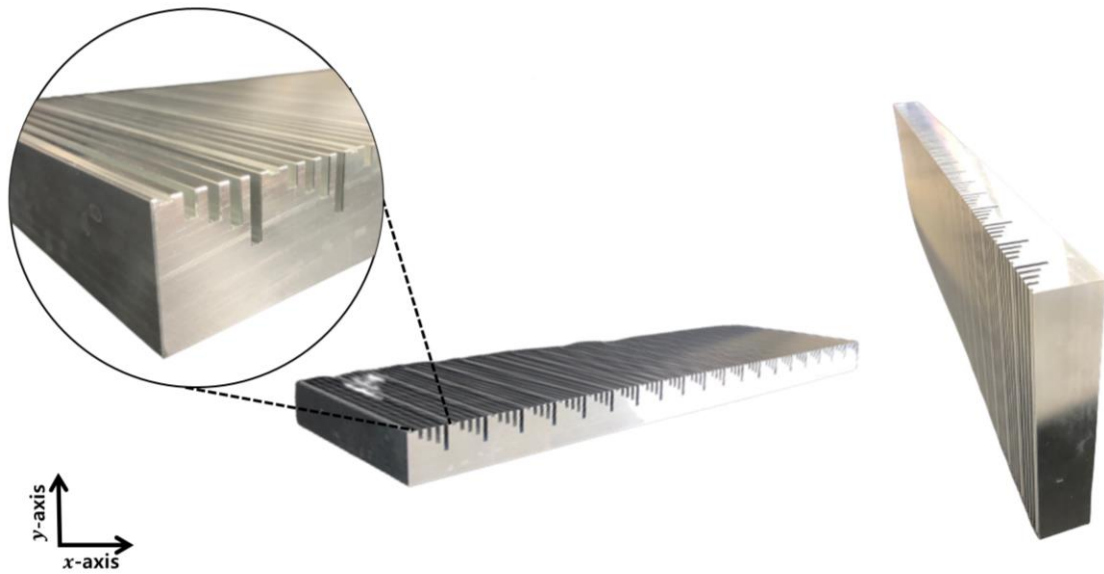


Fig. 3-10 Fabricated metasurface of negative reflection

### 3.3.2 Verify reflection angle

The raw data of the acoustic wave measured in the probed area of Fig 3-8 were summarized and imaged through MATLAB. As a result, we could obtain the results of Fig 3-11. Fig 3-11(a) is an image of  $0^\circ$  incident wave, Fig 3-11(b) is a  $15^\circ$  reflection wave, Fig 3-11(c) is a  $30^\circ$  reflection wave, and Fig 3-11(d) is a  $45^\circ$  reflection image. Although there was a phenomenon of scattering due to experimental error, it is a sufficient result to experimentally show that the reflection angle is controlled according to the design based on the theory.

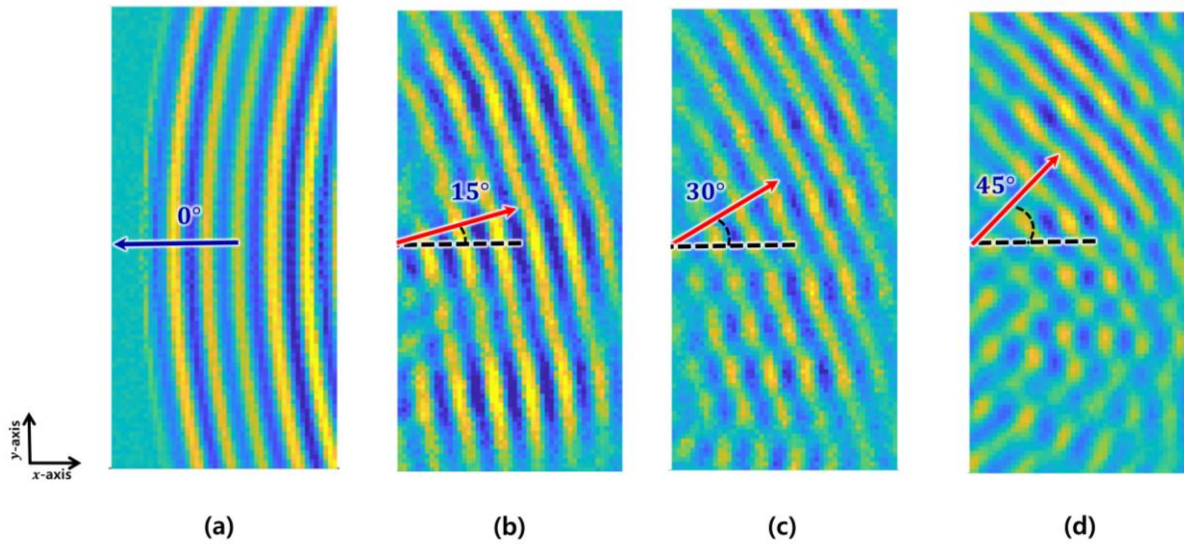


Fig. 3-11 Image of the data measured by probe (a) Incidence  $0^\circ$  (b) Reflection  $15^\circ$  (c) Reflection  $30^\circ$  (d) Reflection  $45^\circ$

### 3.3.3 Negative reflection

Fig 3-12(a) is  $-20^\circ$  incident wave. It looks the same as  $0^\circ$  incidence, but by rotating the metasurface by  $20^\circ$ , it was able to realize the  $-20^\circ$  incidence condition by overcoming the size limitation issue of the water tank. Fig 3-12(b) is an image that the acoustic wave is reflected at an angle  $60^\circ$ . In Fig 3-12(b), a certain part of the scattering effect exists, but it can be sufficiently improved by controlling the thickness and material of the meta structure.

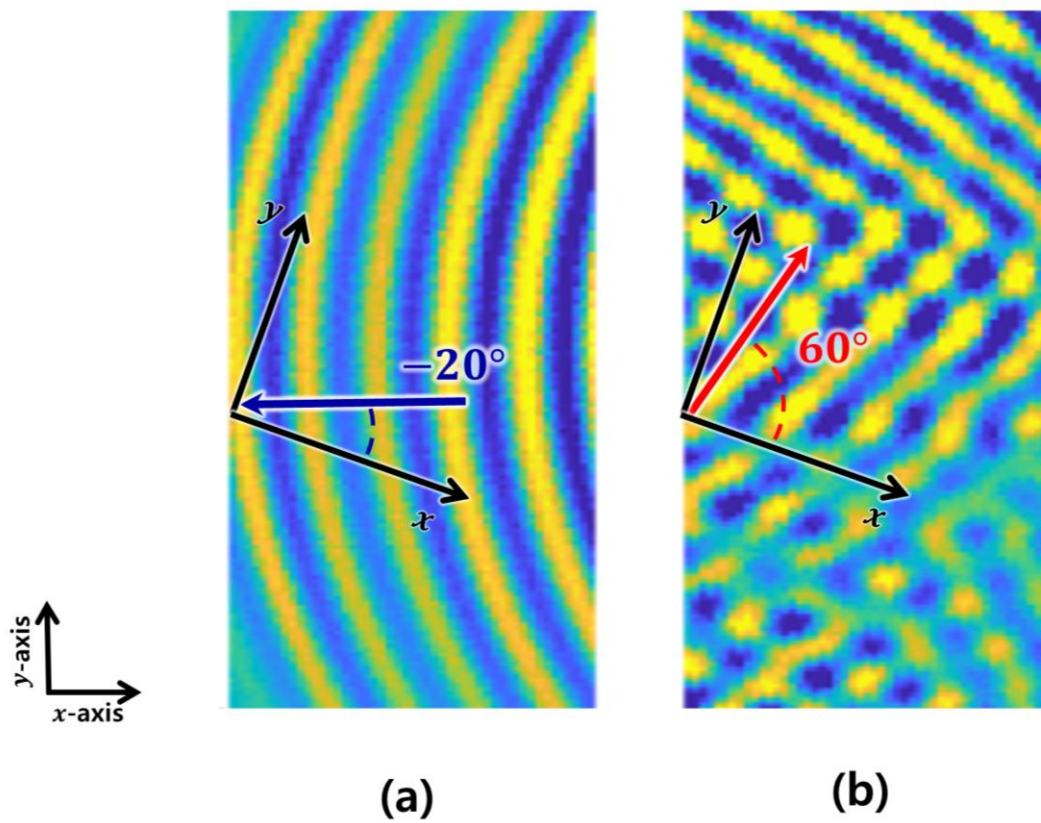


Fig. 3-12 Image of the data measured by probe (a) Incidence  $-20^\circ$  (b) Reflection  $60^\circ$

## 4. Energy dissipation

### 4.1 Theoretical development and structure design

In this section, based on the theory described in section 2.1, 2.2, 2.3, 2.4, and 2.5, I designed a metasurface that dissipate acoustic wave energy and work as if no reflections occurred. Higher order mode conversion by diffraction was implemented by using the metasurface that has large phase gradient. Based on this phenomenon, the principle of maximizing the dissipation of acoustic energy was implemented by designing a metasurface combine with a PDMS that has a large loss factor.

#### 4.1.1 Design the large phase gradient metasurface

In this section, I will design a metasurface with a larger phase gradient than metasurface designed in section 3. If the angle of incident wave is  $0^\circ$ , through Eq. (2-31), the minimum phase gradient value to become a surface wave is 221.6rad/m. We need to design a metasurface wiith a phase gradient larger than 221.6rad/m. In this study, we are going to design a metasurface with a phase gradient of 523.6rad/m. According to Eq. (2-37), it can be seen that the length of the supercell is less than 0.012m, and in order to properly control the thickness of the metaunit, four meta structures of 0.003m will be connected and defined as one supercell. Metasurface could be designed in the same process with section 2.3, and the result is shown in Fig 4-1. Fig 4-1(a) shows the process of measuring the phase change rate according to the length of the meta unit using the two points method. The result is shown in Fig 4-1(b), and the length of the unit length required to divide the thickness of supercell causing the phase change of  $2\pi$  into four is 0.001m, 0.0045m, 0.0055m, and 0.012m as shown is Fig 4-1(c)

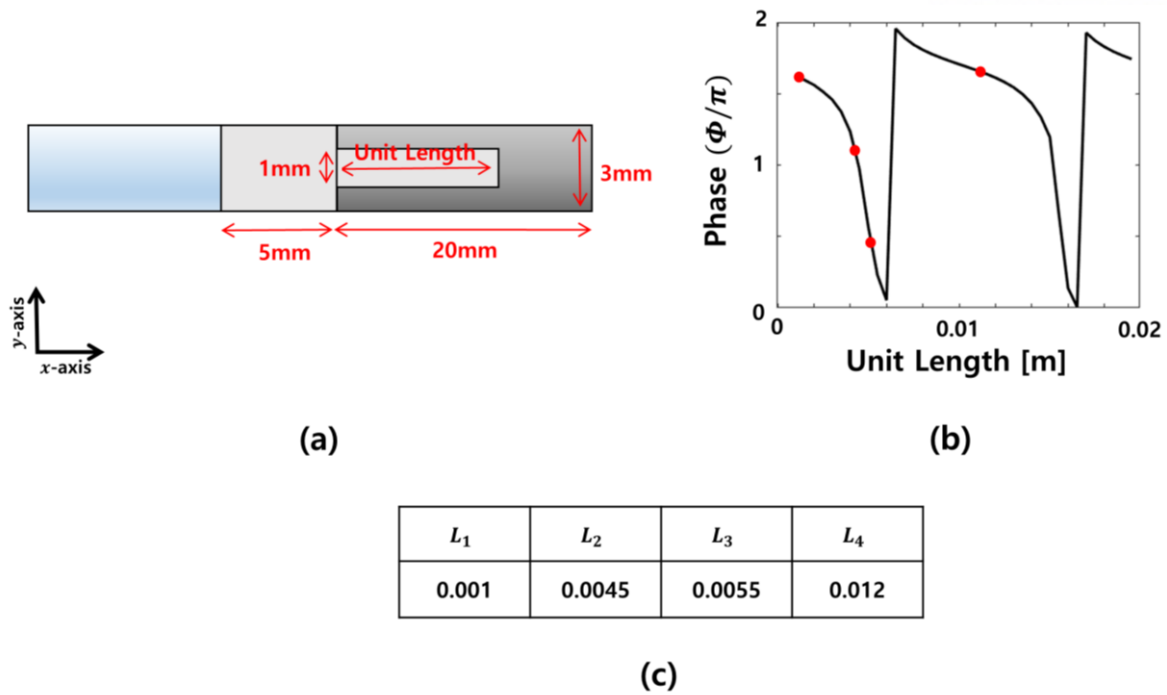


Fig. 4-1 (a) Meta structure unit using for two points method (b) Phase gradient graph according to change of unit length (c) Selected unit length to realize the higher order mode conversion by diffraction

## 4.2 Simulation

In this section, we will check the performance of the metasurface through two simulations using the metasurface structure designed in section 4.1. The first simulation is a frequency response simulation that allows you to check the amplitude of the reflected acoustic wave when it was excited with 50kHz. The second simulation is a transient simulation, which allows you to observe the simulation process from start to end in every  $2\mu s$ .

### 4.2.1 Simulation setting

Let's explain detail about simulation setting. Following the Fig. 4-2, we can place the specimen and experimental equipment. Different with previous experiment, point probe will be used, described as the red point. As we can see, wave will be actuated from right side by 50kHz and amplitude of 1Pa. Yellow line is the condition for "Radiation". Radiation condition is same effect with "No reflection" and it is use for eliminating the reflection that can be the error factors.



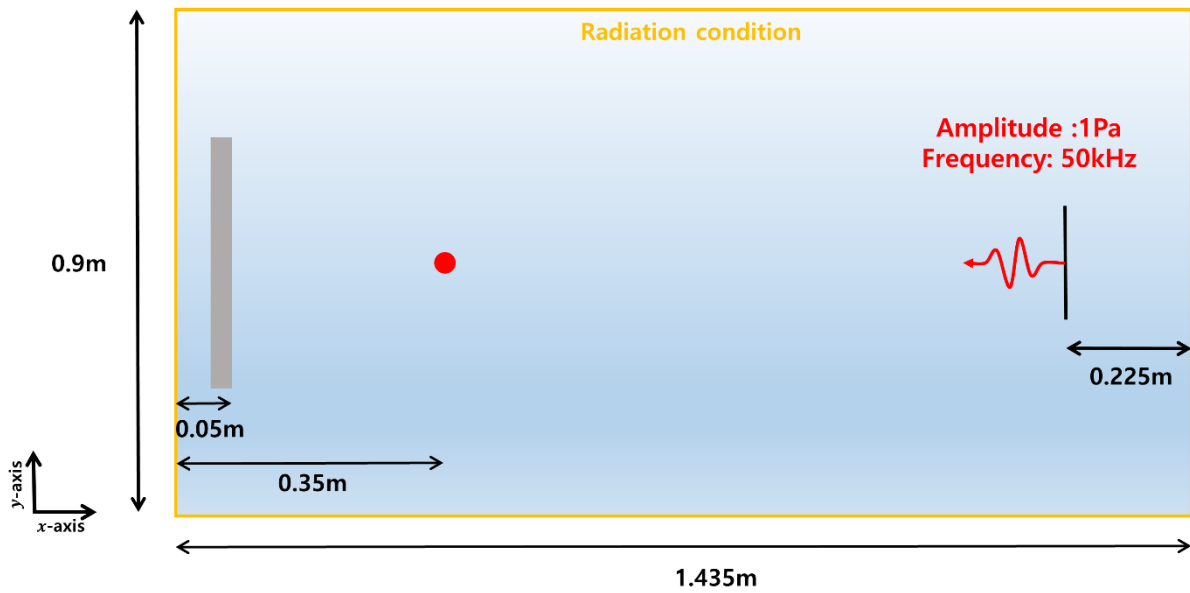


Fig. 4-2 Setting of the simulation

#### [Setting PDMS]

The most important process is setting the PDMS for the material. As PDMS is kind of silicone type material, it has different process to give material property in “COMSOL Multiphysics”. For example, generally when we give material property to the normal solid material, we just select the suitable material and apply it to the geometry we want. However, PDMS is “Rheological material” that shear modulus change according to the frequency and deflection, so we need to define the pressure wave speed and shear wave speed as the Fig. 4-3. Then, we should change the setting of “Linear Elastic Material” from “Young’s modulus and Poisson’s ratio” to the “Pressure wave and Shear wave speed. This is process of changing the properties that define the material from normal solid to the rheological materials.



Parameters			
Name	Expression	Value	Description
Z0	$0.99[\text{MPa} \cdot \text{s} \cdot \text{m}^{-1}]$	9.9E5 Pa-s/m	Characteristic impedanc...
rho0	$970[\text{kg}/\text{m}^3]$	970 kg/m <sup>3</sup>	Density, PDMS
cp0	Z0/rho0	1020.6 m/s	Pressure wave speed of s...

(a) Pressure wave speed

Variables			
Name	Expression	Unit	Description
mu0	$0.6[\text{MPa}] + \text{freq} \cdot 0.7[\text{Pa}/\text{Hz}]$	Pa	Shear modulus, PDMS
cs0	$\text{sqrt}(\text{mu0}/\text{rho0})$	m/s	Shear speed of sound, P...

(b) Shear wave speed

Fig. 4-3 (a)Parameter setting for the pressure wave speed (b)Variable setting for shear wave speed

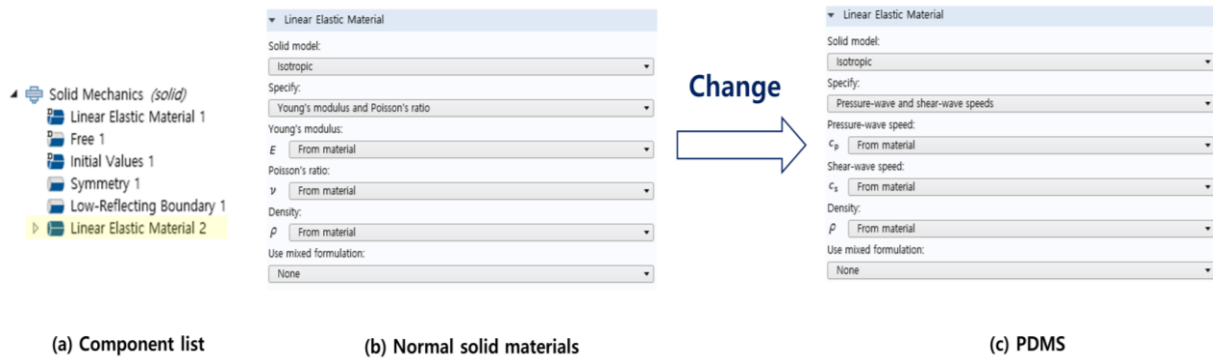


Fig 4-4 (a) Component list of COMSOL Multiphysics (b) Material setting for the normal solid materials (c) Material setting for PDMS by using the wave speed

#### 4.2.2 Frequency response simulation

Based on simulation setting described in section 4.2.1, let's check the acoustic wave dissipation performance of the metasurface with frequency response simulation. Fig 4-5 is the result of simulation that incident wave and reflection wave from the normal surface, and Fig 4-6 is the simulation result of the wave from metasurface structure that designed in section 4.1. As shown in Fig 4-5(a), the distance between the excitation point and the specimen is pretty far, and the magnitude of the acoustic wave measured in front of the structure is 0.55Pa because of the Huygens principle. It can be seen that the size of the

acoustic wave reflected from the normal surface is 0.4Pa and the reduction rate of amplitude is 27%, and the energy reduction rate is 47%. In Fig 4-4 amplitude of incident wave is 0.55Pa that same with the normal surface, and it reflect out with amplitude 0.1Pa. From this, it can be seen that the reduction rate of amplitude is 81% and the energy reduction rate is 97%. Through this results, we can know that the energy dissipation rate of the metasurface has been amplified by more than two times than normal surface.

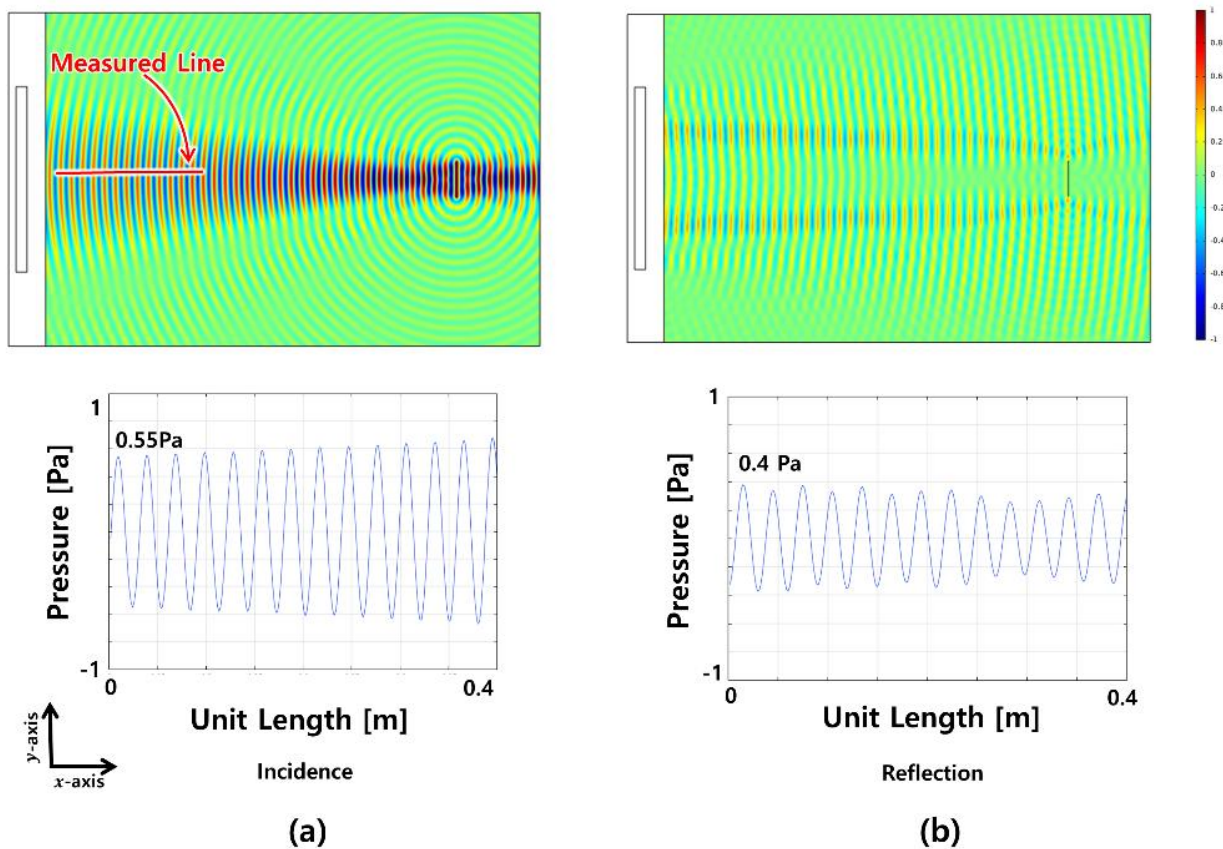


Fig. 4-5 (a) Incidence wave to normal surface (b) Reflection wave from normal surface

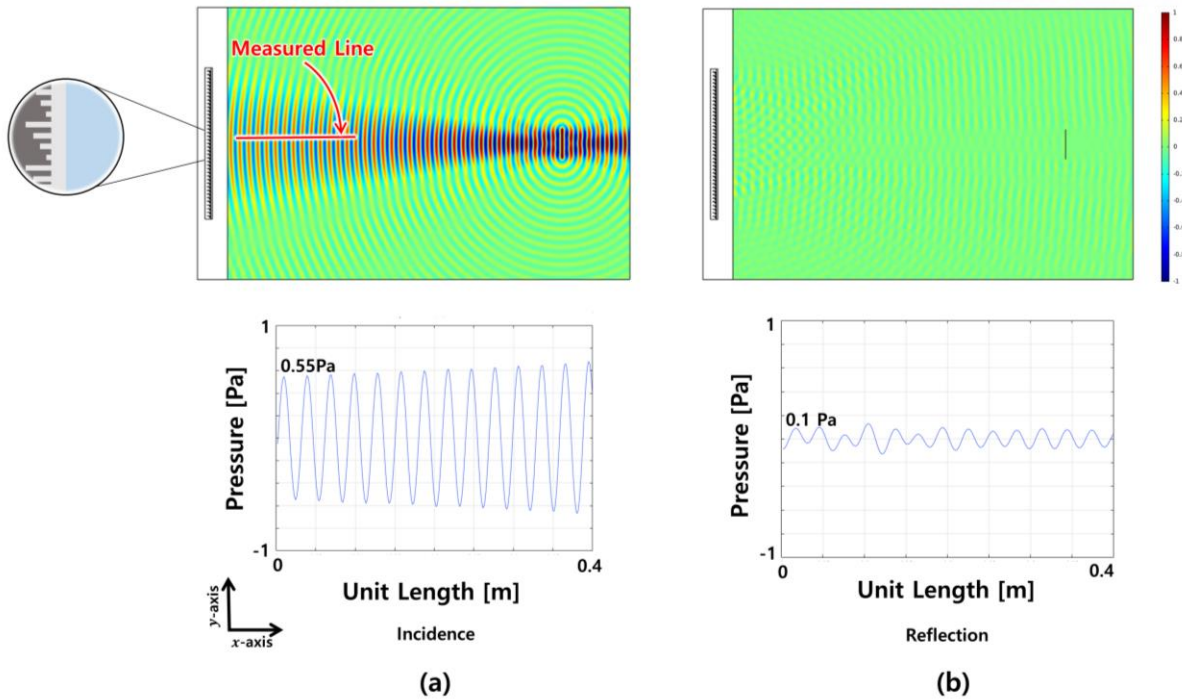


Fig. 4-6 (a) Incidence wave to meta surface (b) Reflection wave from meta surface

#### 4.2.3 Transient simulation

There are two reasons for the amplification of the energy dissipation rate in the metasurface. First, due to the influence of the high phase gradient, the phenomenon that the acoustic wave stays on the surface of the metasurface structure for a certain period of time occurred. Second, as kinetic energy is lost due to friction, during that time, acoustic wave travel along the metasurface and energy dissipation is maximized due to the influence of PDMS, which has a higher loss factor than water. The second is a phenomenon due to the properties of the material, but the first is a phenomenon due to the effect of the structural design, so let's confirm once again through simulation. Transient analysis was performed to confirm time delay, and all conditions are the same as frequency response simulation, but there are differences in that it has only 5 wavelengths and that the probe located 0.35m from the metasurface to measure the acoustic wave. In this simulation, in order to reduce the influence of PDMS, simulation was performed with the metasurface that removed the PDMS as shown in Fig 4-7(a). The result is as shown in Fig 4-7(b), and it can be seen that the time difference does not occur as expected.

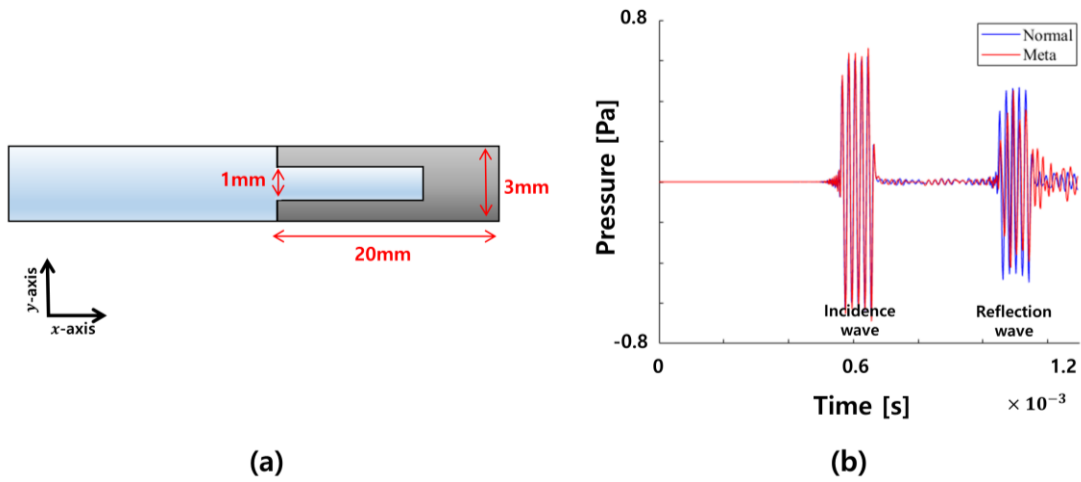


Fig. 4-7 (a) Meta structure unit using for two points method (b) Measured incidence/reflection wave at the probe

For accurate data analysis, as shown in Fig 4-8, FFT analysis was applied to total, incidence, and reflection wave.

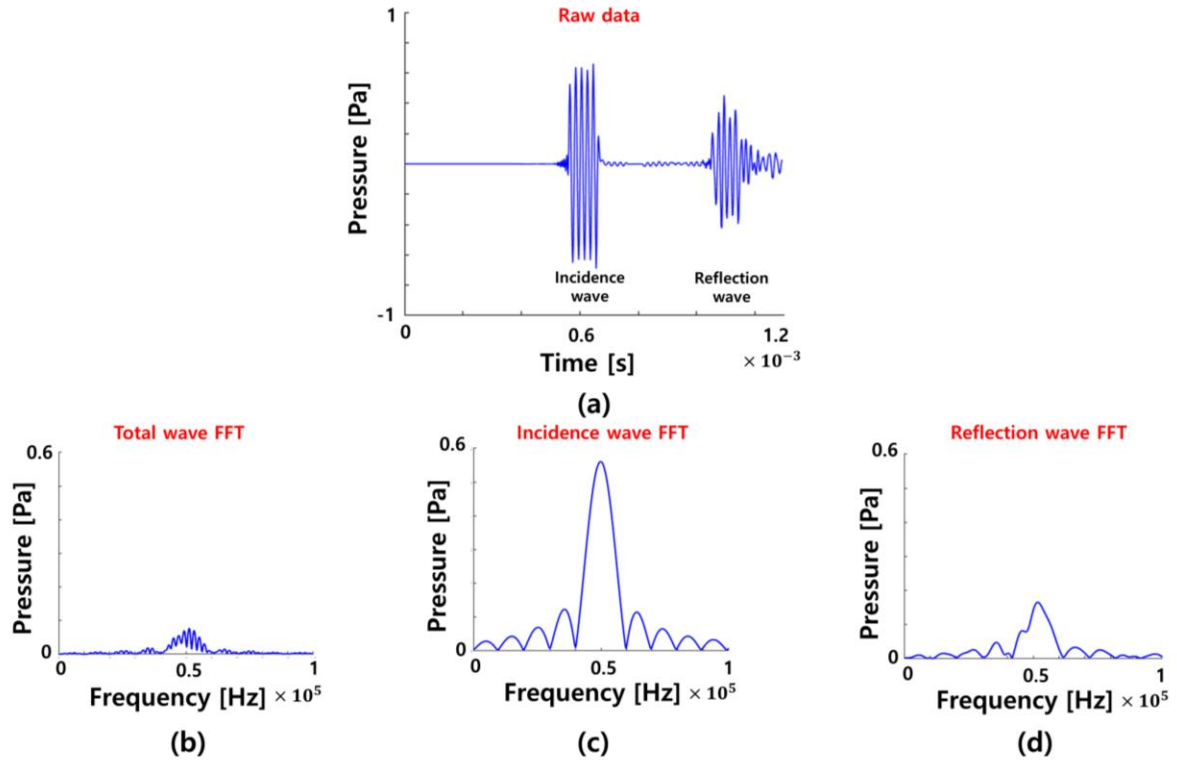


Fig. 4-8 (a) Raw data measured at probe (b) FFT for total wave (c) FFT for incidence wave (d) FFT for reflection wave

It can be seen that the FFT for the whole raw data as shown in Fig 4-8(a) occurs not only at the first 50kHz, but also the frequencies of other bands as shown in Fig. 4-8(b). This can be

interpreted as being affected by simultaneous occurrence of multiple frequencies as well as 50kHz due to the characteristics of transient simulation, unlike the frequency response analysis in which an accurate 50kHz wave is excitation. In addition, it is presumed that various waves are partial overlapped due to various influences such as the nonlinearity of water, vibration of the metasurface due to acoustic wave, and the bending deformation occurring in the thin meta structure.

As shown in Fig. 4-8(c), as a result of FFT for only incident waves, it can be seen that 50kHz is very dominant. However, in Fig 4-8(d), where FFT was performed for only the reflected wave, it can be seen that the dominant wave exists not only the 50kHz buy also the 55kHz to 60kHz band. There are various causes, but in this paper, in order to check the influence of bending deformation occurring in thin meta structures, the time delay simulation was performed with a metasurface with a phase gradient of 255.7rad/m and thickness of the structure was increased.

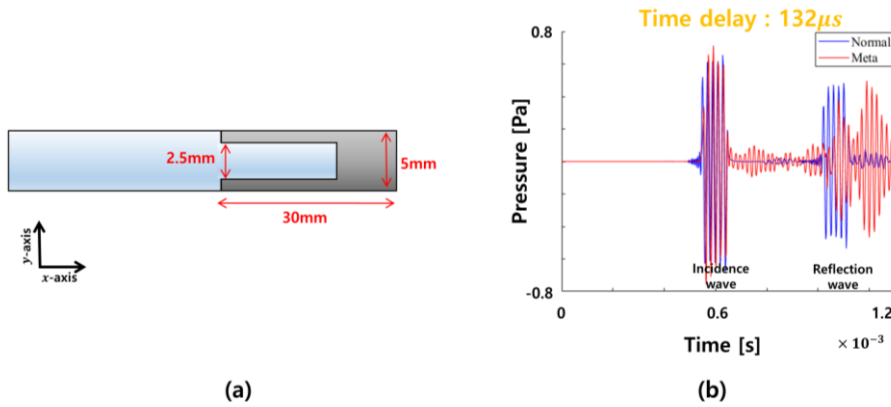


Fig. 4-9 (a) Meta structure unit using for two points method (b) Simulation result of time delay occurred between normal surface and metasurface.

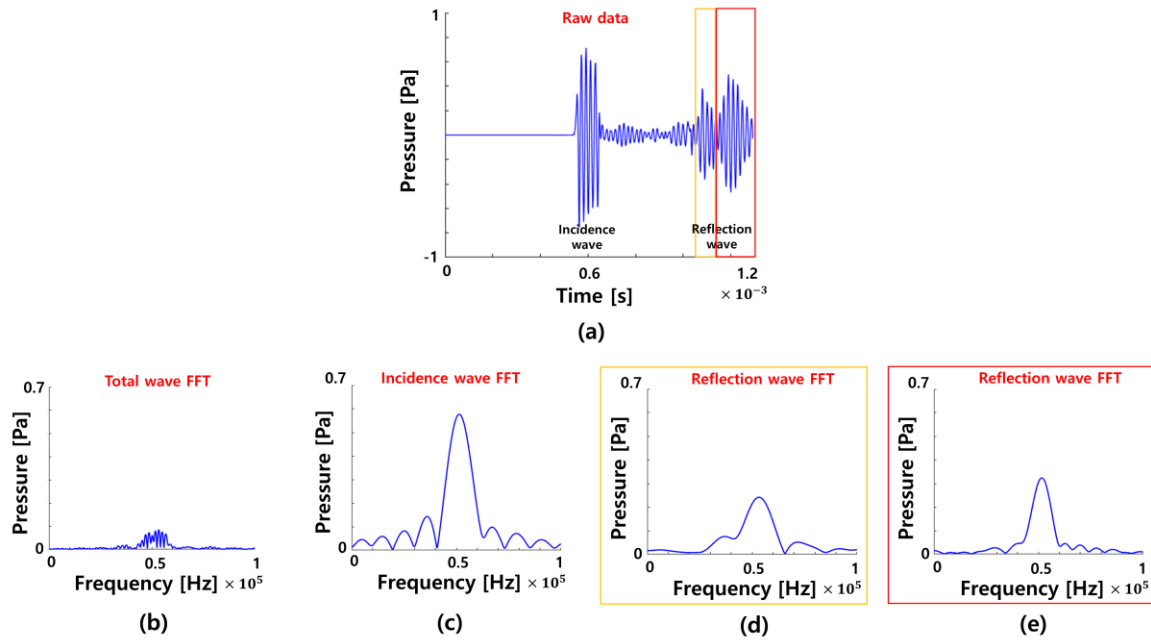


Fig. 4-10 (a) Raw data measured at probe (b) FFT for total wave (c) FFT for incidence wave (d) FFT for first reflection wave (e) FFT for second reflection wave

As shown in Fig 4-9(a), a metasurface unit with a reduced phase gradient was used, and as a result time delay was occurred for  $132 \mu s$  as shown in Fig 4-9(b). From Fig 4-10(a), it can be seen that the reflected wave comes out as two wave forms. To analyze each wave, FFT was performed on the total wave, incidence wave, first reflection wave, and second reflection wave respectively. The results are shown as Fig 4-10 (b), Fig 4-10 (c), Fig 4-10(d), Fig 4-10(e). It can be seen that only 50kHz is overwhelmingly dominant in the incidence wave, however, there are some distortion occurred in both the raw data and the first reflection wave. The first waveform has a wider frequency band than 50kHz, but the second waveform has a very dominant on 50kHz. This is though to be due to the limitations of the transient simulation that mentioned in previous section and also additional factors such as bending, shaking by acoustic wave and reflection from the inside of metasurface. For a more accurate confirmation, I tried to verify the simulation proceeded in Fig 4-9 through an actual experiment. The result is shown in Fig 4-11, and it can be confirmed that there is a time delay of  $72 \mu s$ . It can be seen that the gap between experiment and simulation is very small.

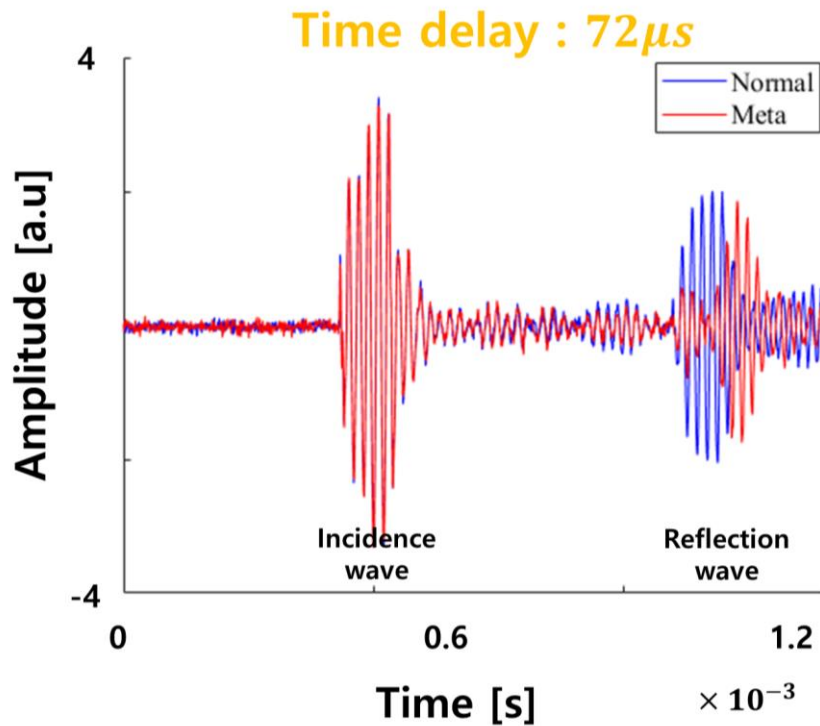


Fig. 4-11 Experimental result of time delay between normal surface and metasurface

As a result, it was confirmed that the higher order mode conversion by diffraction occurs in the metasurface with large phase gradient, and this causes time delay phenomenon. However, in the metasurface with a phase gradient of 523.6rad/m previously proposed, it was not possible to accurately measure the time difference due to external factors and various variables. In the future, more accurate causes will be found through research.

### 4.3 Experimental validation

Metasurface proposed from section 4.1 was confirmed that most of the incident wave energy was dissipated due to the effect of the time delay and the loss factor of the PDMS. In this section, let's check its performance through actual experiment. The experimental equipment and settings are exactly the same as in Fig 3-7 and Fig 3-8, and the arrangement of each equipment and metasurface is exactly the same as in Fig 4-2.

#### 4.3.1 Experimental result

<Specimen metasurface>



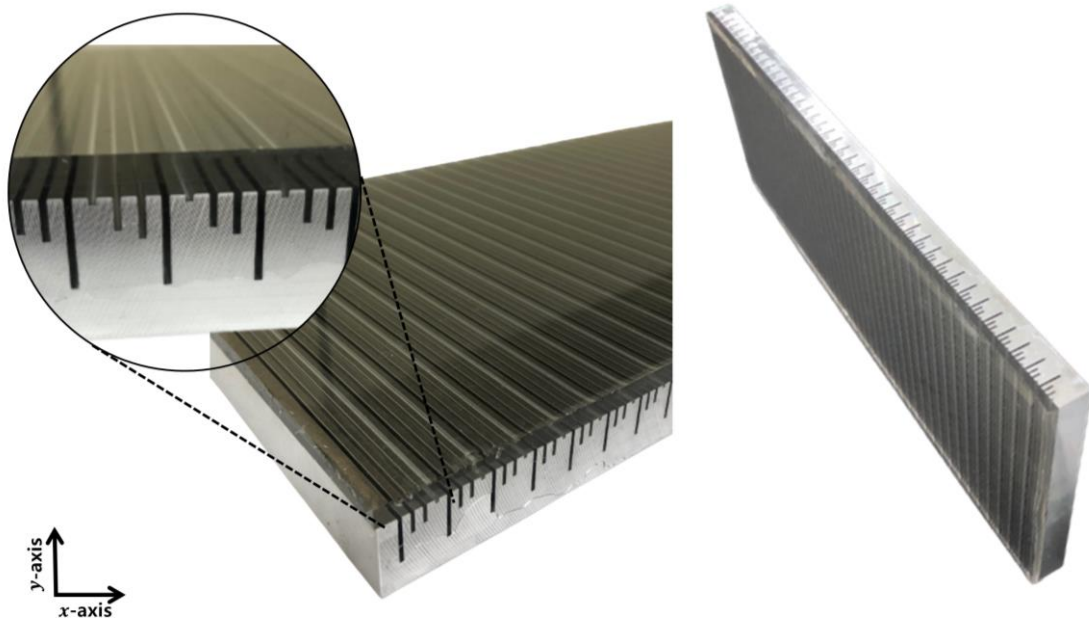


Fig. 4-12 Fabricated meta surface combined with PDMS

The metasurface combined with PDMS that designed in section 4.1.1 was actually fabricated. Using this, the performance of the metasurface was experimentally verified through the following process.

The red point in Fig 4-2 is the location of the probe that measuring the acoustic wave. Among the measured raw data, the incidence wave and the reflection wave were analyzed by FFT and compared their size. Fig 4-13 is the result of the experiment with normal surface, and it was found that the magnitude of the incident wave and the reflected wave was not different that much even with the raw data of Fig 4-13(a). The result of the FFT analysis of the incidence wave and reflection wave are Fig 4-13(b) and Fig 4-13(c) respectively, and the sizes are 0.1 and 0.09 each. That is, if an incident wave with an amplitude of 0.1 is reflected from a normal surface, it can be seen that the amplitude of reflection wave is 0.09. Through this, it can be seen that amplitude reduction ratio is 10% and energy reduction ratio is 19% in normal surface.

Fig 4-14 is the experimental result of metasurface with PDMS and having phase gradient of 523.6rad/m. As shown in Fig 4-14(a), it can be seen that the size of the reflected wave is significantly reduced compared to the incident wave. Fig 4-14 (b) and Fig 4-14(c) are the result of FFT conversion of the incidence wave and the reflection wave respectively. Through this, it can be seen that when incidence wave with amplitude 0.1 reflect from metasurface, reflection wave with amplitude only 0.033 comes out. It can be seen that the amplitude reduction ratio is 67% and the wave energy reduction ratio is 89% from the



proposed metasurface. Compared with the normal surface, it can be seen that the metasurface have 6.5 times in amplitude dissipation rate and 4.5 times in wave energy dissipation rate.

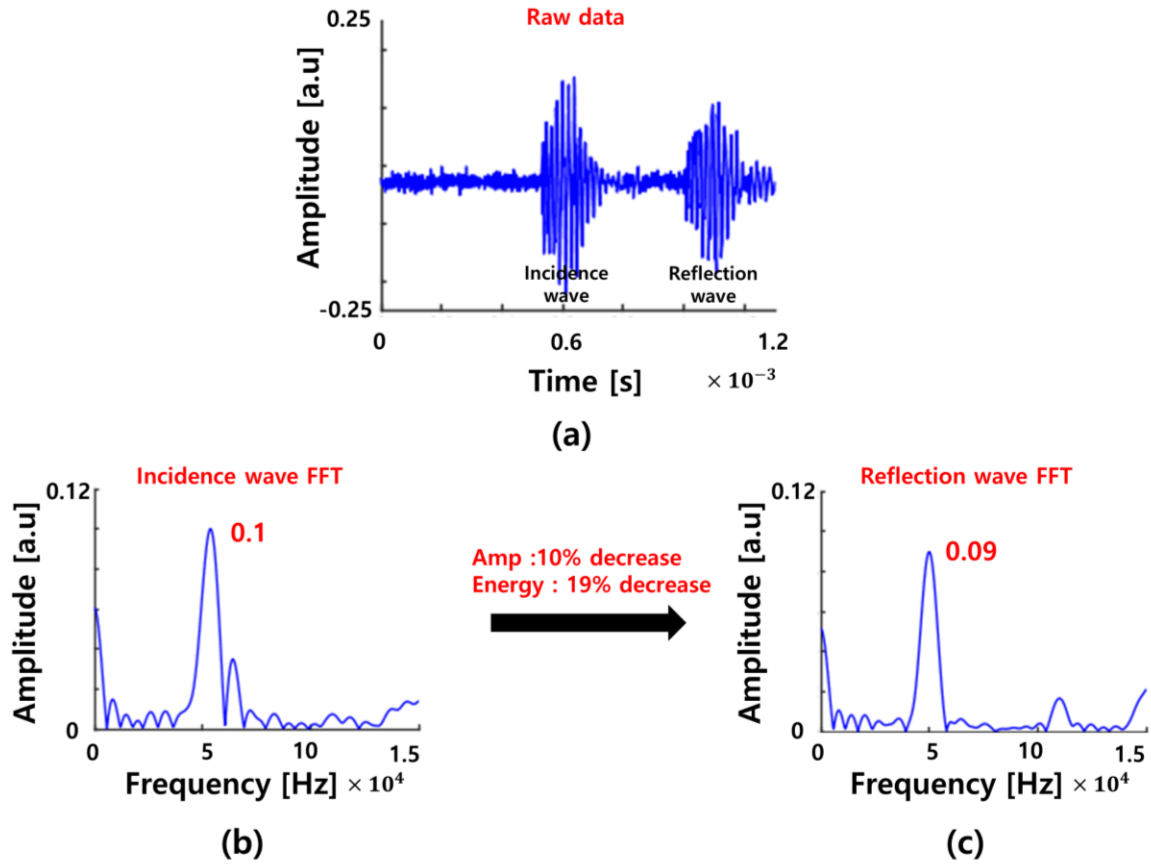


Fig. 4-13 (a) Raw data from experiment with normal surface (b) FFT result of incidence wave (c) FFT result of reflection wave

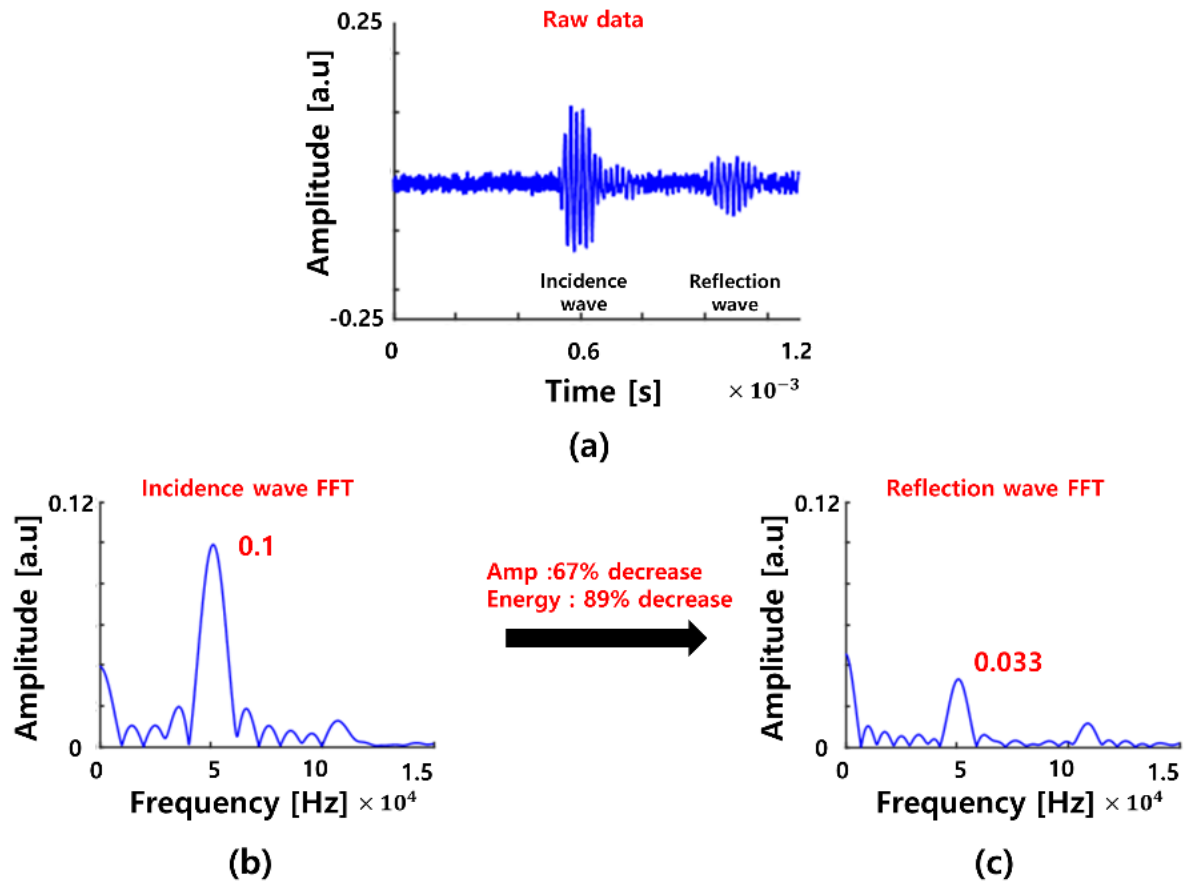


Fig. 4-14 (a) Raw data from experiment with meta surface (b) FFT result of incidence wave (c) FFT result of reflection wave

## 5. Conclusion

In this paper, two acoustic metasurface technologies that can be applied for the stealth technology have been proposed. The first technology is a skill of manipulating the reflection angle using metasurface, and the second is an energy dissipation skill through higher order mode conversion phenomenon.

The metasurface was designed through a theoretical approach using the background theories such as wave equation in acoustic field, Snell's law, higher order mode conversion, two points method, and phase gradient. Performance of designed metasurface was verified through not only simulation but also actual experiments.

The first technology, manipulating the reflection angle, showed that it is possible to implement not only controlling the various reflection angles, but also negative reflection phenomenon that is kind of dynamic control. Also, I could design various metasurface according to my intention. In the second technology, energy dissipation, a special material called PDMS was used to increase the energy dissipation rate, and at this time a special phenomenon called higher order mode conversion was utilized to realize the time delay phenomena, and as a result I could design metasurface having 89% energy dissipation ratio.

The biggest feature of this paper is that it implements the metasurface technology not only in the air but also in the water. There are some differences between representative acoustic media, water and air. First, as the speed of wave is different following the media, depends on the using frequency, structure geometry also being effected. So, if we want to use same range of frequency, metastructure at the air require smaller geometry. Second, water has relatively large acoustic impedance than the air. For this reason, unlike the air, perfect reflection do not occur accurately at the interface of the water and structure. As it doesn't work as hard wall condition in simulation, there are some difference and error can be occur between simulation result and experimental result.

In this research I could design the targeted metasurface and also realize performance through simulation and experiment. Proposed in this paper are applicable to realize underwater stealth technology, which has been actively researched recently, and also can be applied to various acoustic fields such as ultrasound, medical devices, and nondestructive testing

## 6. References

- [1] Zhang, X., & Liu, Z. (2004). Negative refraction of acoustic waves in two-dimensional phononic crystals. *Applied Physics Letters*, 85(2), 341-343.
- [2] Hladky-Hennion, A. C., Vasseur, J. O., Haw, G., Croënne, C., Haumesser, L., & Norris, A. N. (2013). Negative refraction of acoustic waves using a foam-like metallic structure. *Applied Physics Letters*, 102(14), 144103.
- [3] Liu, B., Zhao, W., & Jiang, Y. (2016). Apparent negative reflection with the gradient acoustic metasurface by integrating supercell periodicity into the generalized law of reflection. *Scientific reports*, 6(1), 1-9.
- [4] Wang, W., Xie, Y., Popa, B. I., & Cummer, S. A. (2016). Subwavelength diffractive acoustics and wavefront manipulation with a reflective acoustic metasurface. *Journal of Applied Physics*, 120(19), 195103.
- [5] An, X., Fan, H., & Zhang, C. (2018). Elastic wave and vibration bandgaps in two-dimensional acoustic metamaterials with resonators and disorders. *Wave Motion*, 80, 69-81.
- [6] Zheludev, N. I. (2008). What diffraction limit?. *Nature materials*, 7(6), 420-422.
- [7] Zhang, X., & Liu, Z. (2008). Superlenses to overcome the diffraction limit. *Nature materials*, 7(6), 435-441.
- [8] Leibacher, I., Schatzer, S., & Dual, J. (2014). Impedance matched channel walls in acoustofluidic systems. *Lab on a Chip*, 14(3), 463-470.
- [9] Leroy, V., Strybulevych, A., Lanoy, M., Lemoult, F., Tourin, A., & Page, J. H. (2015). Superabsorption of acoustic waves with bubble metascreens. *Physical Review B*, 91(2), 020301.
- [10] Qi, S., & Assouar, B. (2018). Ultrathin acoustic metasurfaces for reflective wave focusing. *Journal of Applied Physics*, 123(23), 234501.

## 7. Acknowledgement

I appreciate my advisor, Professor. Joo Hwan Oh. Thank you for always try hard to giving me good opportunity to experience various fields and research. Whenever I am mentally shaken, your sincere advice helps me to go in right direction not only in academic field but also in my whole life and it was very helpful. Being taught and get the Master degree from Professor. Joo Hwan Oh must be great luck for me.

I also appreciate my committee member, Professor. Sung Youb Kim. From undergraduate course, I could learn a lot of academic knowledge by your high quality lectures. Also, by seeing how you treat the students sincerely with respect and consideration I could realize the reason that professor is highly respected from a lot of students.

I also appreciate my committee member, Dr. Won Jae Choi. Whenever I have problem in research, I could overcome the difficulties by your advice. Without your motivation and support, I would not have been able to success in my research safely.

I am also thankful to my laboratory members in WAV Lab; Sung Won Lee, Hong Woo Park, Ye Jeong Shin, Sung Bo Kang, Seung Han Kim, and Nam Jung Kim. Special thanks to Geun Ju Jeon about helping me a lot while doing the experiment. Their supports and knowledge helped me a lot to develop research.

Dear the most important to my family and my friends; Min Jae Kim and Young Hoon Jung, I would like to give sincere appreciation to them.

I dedicate this thesis to my advisor, committee members, laboratory members and my family and friends for their supports.

